


Cite this: *RSC Adv.*, 2023, 13, 1787

Stability of perovskite solar cells: issues and prospects

Tanzi Ahmed Chowdhury,^a Md. Arafat Bin Zafar,^a Md. Sajjad-Ul Islam,^{ID a}
M. Shahinuzzaman,^{ID *b} Mohammad Aminul Islam^{*c}
and Mayeen Uddin Khandaker^{*de}

Even though power conversion efficiency has already reached 25.8%, poor stability is one of the major challenges hindering the commercialization of perovskite solar cells (PSCs). Several initiatives, such as structural modification and fabrication techniques by numerous ways, have been employed by researchers around the world to achieve the desired level of stability. The goal of this review is to address the recent improvements in PSCs in terms of structural modification and fabrication procedures. Perovskite films are used to provide a broad range of stability and to lose up to 20% of their initial performance. A thorough comprehension of the effect of the fabrication process on the device's stability is considered to be crucial in order to provide the foundation for future attempts. We summarize several commonly used fabrication techniques – spin coating, doctor blade, sequential deposition, hybrid chemical vapor, and alternating layer-by-layer. The evolution of device structure from regular to inverted, HTL free, and ETL including the changes in material utilization from organic to inorganic, as well as the perovskite material are presented in a systematic manner. We also aimed to gain insight into the functioning stability of PSCs, as well as practical information on how to increase their operational longevity through sensible device fabrication and materials processing, to promote PSC commercialization at the end.

Received 19th September 2022
Accepted 15th December 2022

DOI: 10.1039/d2ra05903g

rsc.li/rsc-advances

1. Introduction

Consumption of electricity is a necessary part of modern living. Global power demand has continued to rise at a higher rate than global energy production. Currently, fossil fuels such as oil, coal, and gas are used as convenient sources to generate electricity. Overall, these fossil fuels are defined as non-renewable sources of energy, meaning their reserves will be run out after a certain period. Furthermore, the energy conversion process from these sources releases a significant amount of carbon to the dwelling environment which creates a greater risk for our existence.¹ Thus, the transformation from fossil fuel-based energy to clean, green, and renewable sources

of energy is a critical issue and has a great demand. Undoubtedly, for the betterment of the world, it is vital to adopt environmentally friendly technology together with renewable energy sources. Albeit, the development of various technology relevant to energy conversion and management is at pace for different natural and renewable energy resources, such as wind, solar, hydro, biomass, *etc.* However, among them, solar photovoltaic (PV) technology is considered to be the most effective and promising renewable energy technology. Particularly, solar energy is the most profuse renewable energy source on the planet. An approximate estimation shows that the sun emits solar radiation at a rate of 3.8×10^{23} kW s⁻¹, of which the earth uses only a minute amount of 1.8×10^{14} kW s⁻¹.¹ The amount of solar energy that strikes the earth per day is sufficient for the current world population to consume it in 27 years.² This fact indicates that solar energy is extensively applicable on a small (household level) to large scale (industry standard). Currently, renewable energy sources generated 26% of the total 26 615 TW h of worldwide electricity output in 2019, with solar energy accounting for 1.9%.³ Solar PV cells can directly convert light energy into electricity without any interface. Solar PV uses less power, delivers more, and is easy to handle because of less complexity. The solar PV industry is a vast field with many types of solar cells which is divided into several generations. These are the first generation-wafer based solar cells such as single

^aDepartment of Electrical & Electronic Engineering, Faculty of Engineering, International Islamic University Chittagong, Kumira, Bangladesh. E-mail: ahmedtanzi991@gmail.com; arafatbzafar@gmail.com; sajjadulislam714@gmail.com

^bInstitute of Fuel Research and Development, Bangladesh Council of Scientific and Industrial Research (BCSIR), Dhaka 1205, Bangladesh. E-mail: shahinchmiu@gmail.com

^cDepartment of Electrical Engineering, Faculty of Engineering, Universiti Malaya, 50603 Kuala Lumpur, Malaysia. E-mail: aminul.islam@um.edu.my

^dCentre for Applied Physics and Radiation Technologies, School of Engineering and Technology, Sunway University, 47500 Bandar Sunway, Selangor, Malaysia. E-mail: mayeenk@sunway.edu.my

^eDepartment of General Educational Development, Faculty of Science and Information Technology, Daffodil International University, DIU Rd, Dhaka 1341, Bangladesh



crystal or monocrystalline silicon (c-Si), poly or multi-crystalline silicon (p-Si), the second generation-thin film based solar cells such as cadmium telluride (CdTe), amorphous silicon (a-Si), gallium arsenide (GaAs) and copper-indium-gallium-selenide (CIGS), and the third generation-nanocrystal based solar cells such as copper zinc tin sulfide (CZTS), dye-sensitized solar cells (DSSCs), perovskite solar cells (PSCs), organic photovoltaics (OPVs) and quantum dot solar cells, *etc.* However, there remains a considerable issue concerning the generation and shape of the solar cell, durability, reliability as well as price.^{4,5}

Among the various types of 3rd generation PV devices, the PSCs are received greater attention from the scientific community. In the year 2009, based on the DSSC technology, the PSC was introduced as a potential renewable energy PV technology. In PSCs, key material is the perovskite which formed by the organic-inorganic mixed compound with an ABX₃ crystal structure that works as an active light-harvesting layer. The symbols A and B denote two cations, and X is an anion. Particularly, "A" can be calcium (Ca), cesium (Cs), methylammonium (MA), or formamidinium (FA); "B" can be titanium (Ti), lead (Pb) or tin (Sn), and "X" can be chlorine (Cl), bromine (Br) or iodine (I).⁶ Numerous techniques have been employed for fabricating perovskites material and devices such as spray coating, dip coating, two-step deposition, chemical vapor deposition, ink-jet printing, blade coating, and screen-printing method, *etc.*^{6–18} In the following section of this study, the preparation techniques were shown schematically. Particularly, every technique has shown some advantages and limitations. It should be noted that perovskites are already well recognized for having remarkable and ideal characteristics for solar cell applications, such as a direct bandgap,¹³ absorption over a wide spectrum,¹⁴ high defect tolerance ability and over a micrometer range of charge carrier diffusion lengths.¹⁵ PSC with CH₃NH₃PbI₃ perovskite was first reported in 2009 by Miyasaka *et al.*¹⁶ They used liquid electrolyte as hole transport layer (HTL) to fabricate PSC with TiO₂ scaffold perovskite absorber layer. The reported PCE was 3.8%. However, it is found that perovskites are soluble in these electrolytes, which causes fast deterioration over a short period of time (less than an hour).¹⁷ A major improvement in stability and PCE has been primarily achieved by Kim *et al.* in 2012 using solid state HTL.¹¹ They used spiro-OMeTAD (2,2',7,7'-tetrakis (*N,N*-di-*p*-methoxyphenylamine)-9,9'-spirobifluorene) instead of liquid electrolyte which is commonly used in organic LEDs. The achieved PCE was 9.7% and the device found to be stable for 500 h in room ambient without encapsulation. In the same year, Lee *et al.*¹² reported several key developments include improved PCE up to 10.9%. They fabricated mixed halide perovskite CH₃NH₃-PbI_{3-x}Cl_x and found that the perovskite could transport both electrons and holes. They also replaced TiO₂ scaffold layer with insulating Al₂O₃. Also, the device shows better charge transport properties and higher stability than CH₃NH₃PbI₃ perovskite. Numerous efforts were given by the researcher to improve the PCE and stability of PSCs including structural modification, developing novel materials, and modification of pre- and post-fabrication techniques, *etc.*, which is continuing till today yet to get the expected stable and high efficiency PSCs. Leijtens

*et al.*¹³ were successful in increasing the PCE to 19.1% for monolithic tandem PSC which retained more than 80% of its initial efficiency over 300 hours at 85 °C in air. Akin *et al.* also fabricated a PSC with a PCE of 22% which shows excellent stability over 2000 hours of continuous 1.0 sun illumination.¹⁸ Zhou *et al.*¹⁹ reported that during fabrication, low humidity (RH 30%) regulates the perovskite crystal formation and increases the PCE to 19.3%.

High-efficiency devices with PCE of 20.26% on rigid substrates and 17.41% on flexible substrates have been reported by Chen *et al.*²⁰ in 2018 using Cu doped NiO_x as a HTL. The devices were inverted structure which showed stable performance in ambient conditions with high humidity (50–65%) for 1000 hours. It has also been reported that alkali chloride interface modification of the NiO_x hole transport layer results in improved ordering of the perovskite films, which in turn lowers defect/trap density, lowers interfacial recombination, suppresses ion migration, and increases device stability and efficiency.²¹ According to Song *et al.*, p-p+ homojunctions such as a NiO/Cu:NiO bilayer can increase the PSC's effectiveness, which is unquestionably higher than employing NiO or Cu:NiO alone as HTM. In particular, the homojunction speeds up hole transfer and blocks the electron transport in the HTL, improving hole extraction and stifling carrier recombination at the NiO/perovskite interface simultaneously. With a strong working stability and a PCE of 18.3%, the PSC with bilayer HTM maintained 80% or so after 350 hours.²² Min *et al.* recently fabricated PSCs with highest PCE of 25.8% using inter-layer modification which reduces the interface defects between the SnO₂ ETL and perovskite absorber layer.²³ The devices maintained almost 90% of their initial efficiency after 500 hours of continuous light exposure. Their findings showed that the device efficiency and stability could be improved *via* suppressing the interface defects.

It could be easily realized that the efficiency grew from 3.8% to 25.8% in just a few years, beating numerous established commercial PV technologies like Si, CdTe and GaAs-based solar cells, however, the stability not yet to be comparable with those commercial solar cells. One of the main reasons is that the perovskite materials contain unstable elements due to extra weak interactions such as van der Waals force and weak hydrogen bond.²³ Moreover, the stability of perovskite technology depends on its environmental sectors: humidity, thermal treatment, and lighting.²⁴ According to Bass *et al.*,²⁵ perovskite crystallization might be regulated by humidity. The aforementioned information indicates that the biggest hurdles of a successful perovskite technology are to develop a low-cost manufacturing technique and ensure the long-term stability of the device. We believe that PSCs will be able to dominate the market if these two concerns can be remedied.

The purpose of this review is to provide a comprehensive overview of the structural evolution that influences the stability of perovskite devices. This article is organized into different sections; the main factors that the stability and longevity studies concerning the structure of PSCs have discussed in detail, followed by processing methods. Also, this article has addressed the economic feasibility depending on the current



studies which confirmed that the PSCs are more environmentally and economically sustainable and competitive.

2. Key challenges in stability

The lack of stability of perovskite materials is a well-known issue and it has been shown that at the device level, several degradations occur simultaneously at various interfaces. Moisture, UV light, hot temperatures, and exposure to the outside air can all directly contribute to these degradations. The causes of the stability issue can thus be determined to be intrinsic stability, moisture ingress, oxygen ingress, and illumination accelerated decomposition, just like with other materials composed of organic materials.^{26,27} Intrinsic stability refers to the chemical and structural stability of devices throughout a wide range of photovoltaic working conditions in the presence of contaminants, particularly oxygen and water, which were introduced into the device during production. Extrinsic stability is concerned with the failures of sealing and moisture blocking layers. Under normal conditions, degradation mechanisms are activated or accelerated. The instability issues are shown schematically in Fig. 1. Therefore, the aforementioned conditions may also contribute to the material's disintegration of the organic layer, top electrode instability, photo-degradation, and crystallization instability. Numerous degradations can begin even in the absence of water or oxygen due to the intrinsic deterioration produced by thermal stress or illumination.²⁸ Both the employed charged transport material's instability and the inherent instability of the perovskite material are to blame for the stability's drawbacks.²⁹

One of the key challenges remains in perovskite solar cell fabrication process. We have not yet been able to manufacture high efficiency PSCs on a big scale or in atmospheric conditions. Limitation retained because the fabrication operations

must be completed in a controlled and inert ambient (glove box) as the perovskites are very sensitive to oxygen and moisture.³⁰ Moreover, when the built devices are measured under ambient conditions, severe perovskite deterioration is noted. The unintended decrease in efficiency caused by PSC deterioration may restrict the use of PSCs outside.³¹ There are numerous data on how oxygen and moisture affect the strength and effectiveness of PSCs.³² PSCs are also degraded when exposed to light. In the presence of air and UV radiation, $\text{CH}_3\text{NH}_3\text{I}$ produces a brown colour, which Zhao and his team attributed to the presence of I_2 .³² This I_2 may be comes from the decomposition perovskite materials in presence of air and UV radiation.

In addition to the stability problems related to UV radiation, oxygen, and moisture, the thermal stability of PSCs also causes a lot of concern.³³ Degradation of the perovskite layer can be brought on by exposure to high temperatures. It is crucial to keep in mind that during operation, the solar modules will be subjected to temperatures as high as 100 °C. The impact of higher temperatures on $\text{CH}_3\text{NH}_3\text{PbI}_{3-x}\text{Cl}_x$ and $\text{CH}_3\text{NH}_3\text{PbI}_3$ was researched by Philippe *et al.*³⁴ Since XPS is better suited to analyzing the chemical components of samples regardless of their crystallinity, it was utilized to explain the breakdown of these films. In order to evaluate the sole effect of temperature on the film degradation, the film was heated in an ultra-high vacuum chamber at 100 °C in the absence of air and moisture. The N/Pb and I/Pb proportions discovered by XPS were used to characterise the films. The decline in these ratios illustrates how the perovskite material transforms into lead iodide can be seen elsewhere.³⁴ This elemental study makes it very evident that perovskites cannot withstand temperatures above 100 °C. Additionally, it was mentioned that while being annealed at 85 °C, the $\text{CH}_3\text{NH}_3\text{PbI}$ might disintegrate in an inert atmosphere.³⁵ It has been reported that the XA cation may be responsible for the thermal stability, which may be enhanced by switching the cation element.

Another key challenge is remains to find the best suited carrier transport materials as the stability of a PSC device is significantly influenced by them.³⁶ Using hydrophobic HTM, significant improve in stability has been observed.³⁷ PSCs made with poly(3-hexylthiophene) as the HTM and methylammonium lead iodide bromide ($\text{CH}_3\text{NH}_3\text{PbI}_2\text{Br}$) perovskite showed excellent stability for 250 hours, but the measured efficiency was low (less than 10%).³⁸ To increase the stability of PSC, several dopants, such as iridium complex, have also been proposed.³⁹ According to certain theories, the instability of perovskite solar cells is also caused by corrosive or hygroscopic chemicals employed to increase the conductivity of the hole transport material.⁴⁰ The stability of perovskite solar cells improved when spiro was employed in place of the typically utilized lithium compound LITFSI (TFSI). To minimize the effect of HTM in stability of PSCs, the HTM free PSCs have also been proposed by many researchers. This topic has been discussed details in later section. However, it has been reported that the PSCs without HTM can only keep 35.5% of their efficiency after being stored in ambient conditions for 15 days, the involvement of the HTM layer in the deterioration is likely to be less significant than the intrinsic degradation of the perovskite.⁴¹

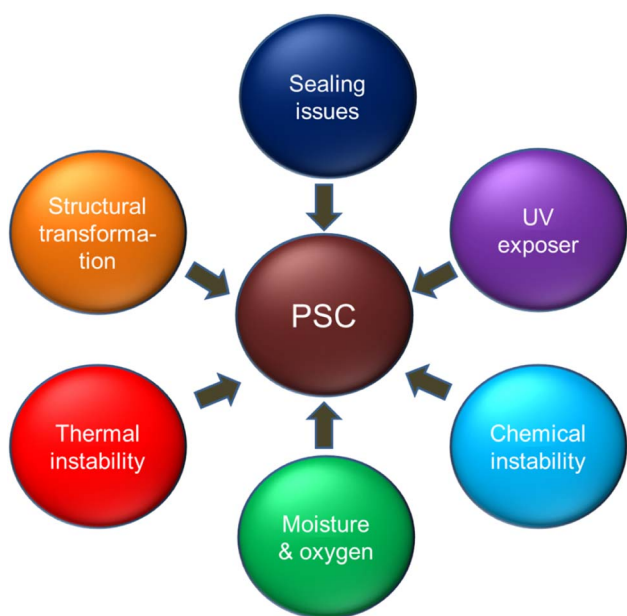


Fig. 1 Several instability issues related to the PSCs.

The using of metal electrodes has also been remaining as a challenge yet to date. The kind of electrode utilized has a significant impact on the chemical stability of perovskite devices.⁴² Due to its possible maximum efficiency, gold (Au) has been widely used as an electrode in modern perovskite devices⁴² even it is rather pricey. To reduce the cost, it has been suggested by Machui and colleagues that silver (Ag) paste can be used instead of Au.⁴³ However, compared to PSCs with Au-based cells, Ag-back electrode PSCs exhibit low environmental stability. It was confirmed that having a hydrophobic electrode or hydrophobic hole transport layer could be advantageous for increasing the stability of PSCs.⁴⁴ While electrodes and hydrophobic transport materials are thought to increase stability, the fabrication techniques for creating the layers may also be effective in terms of stability and productivity which has been discussed in the later section.

Several strategies have yet to be suggested to increase PSC stability. There were numerous suggestions to contain the anomaly for each odd stability problem.⁴⁵ Some suggested that using organometallic halide PSC with a different chemical structure could increase stability.³⁴ They reported that the devices with mixed bromide iodide perovskites, such as methylammonium lead iodide bromide, have been demonstrated to have enhanced moisture stability as compared to pure methylammonium lead iodide devices. Iodide bromide, however, has a greater bandgap than regular $\text{CH}_3\text{NH}_3\text{PbI}$, which results in inferior efficiency when compared to classical devices.⁴⁶ Additionally, it was reported that the increased encapsulation approach may increase stability, however it was found that even at high temperatures, material deterioration persisted.⁴⁷ The following methods have been suggested for tin-based perovskite devices to improve stability and efficiency: (I) TiO_2 replacement with alumina, (II) UV filter application or doping of TiO_2 to reduce UV-induced photocatalysis, (III) use of additives, (IV) replacement of hole transport materials, (V) replacement of the top electrode, (VI) addition of buffer layers, and (VII) development of perovskite material with different molecular structure.³⁵

3. Charge transport layers in PSCs

It should be noted that the type and crystalline structure of perovskite (PSK) and charge transport materials, as well as the device structure, all play important roles in determining device durability. Particularly, a perovskite active layer is sandwiched between an ETL and HTL in a typical high-performance PSC where the ETL and HTL assist the extraction of the light-generated carrier in the PSC. Numerous n-type semiconductor materials have been experimented with as an ETL in PSCs which has been listed in Fig. 2(a). In the case of ETL, it should be remembered that the conduction band of the ETL should be lower than the absorber's, and the absorber's VB (valence band) should be higher than the ETL's for efficient charge extraction.⁴⁸ The interface between the ETL and the perovskite absorber is critical to the device's performance since poor band alignment of the ETL with the perovskite absorber can enhance carrier recombination and have an impact on the device's series and

shunt resistance. To address these issues, materials with good band alignment and high carrier mobility should be carefully chosen to improve electron injection and hole blocking at the ETL/perovskite interface, resulting in high current density (J_{sc}) and device performance.⁴⁹ Fig. 2(b) depicts the many features of an ETL that must be taken into account while constructing high PCE PSC devices. Many techniques are being investigated to find the ideal ETL for PSC use with better mobility, strong thermal stability, low trap density, and low-temperature processability. The HTL, on the other hand, is primarily responsible for transporting holes created in the perovskite layer to the back-contact metal electrode. It also prevents reverse electron transmission by acting as a barrier between the perovskite layer and the counter electrode. It affects the device's V_{oc} (open circuit voltage) by affecting the splitting of the perovskite's quasi-Fermi-energy levels.^{50,51} A perfect HTL would be low-cost, have excellent thermal stability, low electron affinity, strong hole mobility, and be compatible with perovskite energy levels. Several HTLs like polymeric, carbon, small molecules, and inorganic compounds have been identified and examined as HTLs for PSCs as shown in Fig. 2(c), with expected features for higher PCE as illustrated in Fig. 2(d).

Even though this is paradoxical, however, it has been claimed that the inclusion of HTL and ETL layers complicates the fabrication process, affects device stability, and increases the cost. To commercialize this technology, it is crucial that the structure of PSCs be simplified further without losing their photovoltaic performance. As a result, structural modification including ETL-free or HTL-free PSCs is gaining popularity in the research community. In this section, the development of diverse device structures of PSCs is discussed including their PCE and stability, and future perspectives.

4. Structural evolution of PSCs

4.1 Mesoporous PSCs

Mesoporous PSCs are recognized for high PCE,⁵⁰ simple fabrication methods, and low material cost. The mesoporous structure of ETL and the thickness of the active perovskite layer is the main factor in this solar cell. Primarily, a PCE of 9.7% has been achieved for nanocrystal mesoporous MAPbI_3 perovskite material.¹⁰ First, a compact layer, in most cases TiO_2 is deposited on FTO (fluorine-doped tin oxide) coated glass substrate as shown in Fig. 3(a) which causes blocks the holes and brings out the electrons. Then a mesoporous layer, in most cases TiO_2 or Al_2O_3 or mixed of both is deposited on top of the compact layer.⁵² The mesoscopic layer has been fabricated by using several techniques, such as screen printing,⁵³ spin coating, magnetron sputtering,⁵⁴ electrospinning,⁵⁵ etc. Particularly, reducing the thickness of the mesoporous layer gradually increases the PCE.⁵⁶ Kojima *et al.*⁵⁷ is the pioneer in developing a mesoporous PSC using MAPbI_3 and found PCE of 3.8%. Later, Park and Graetzel's group claimed improved PCE of 9.7% by using the liquid-state electrolyte.⁵⁸ A new sandwich-type structure is developed where 3D nanocomposites of mesoporous- TiO_2 with $\text{CH}_3\text{NH}_3\text{PbI}_3$ and polymeric HTMs were used and found a PCE of 12%. With this structure but mixed halide $\text{CH}_3\text{NH}_3\text{PbI}_{3-x}\text{Br}_x$,



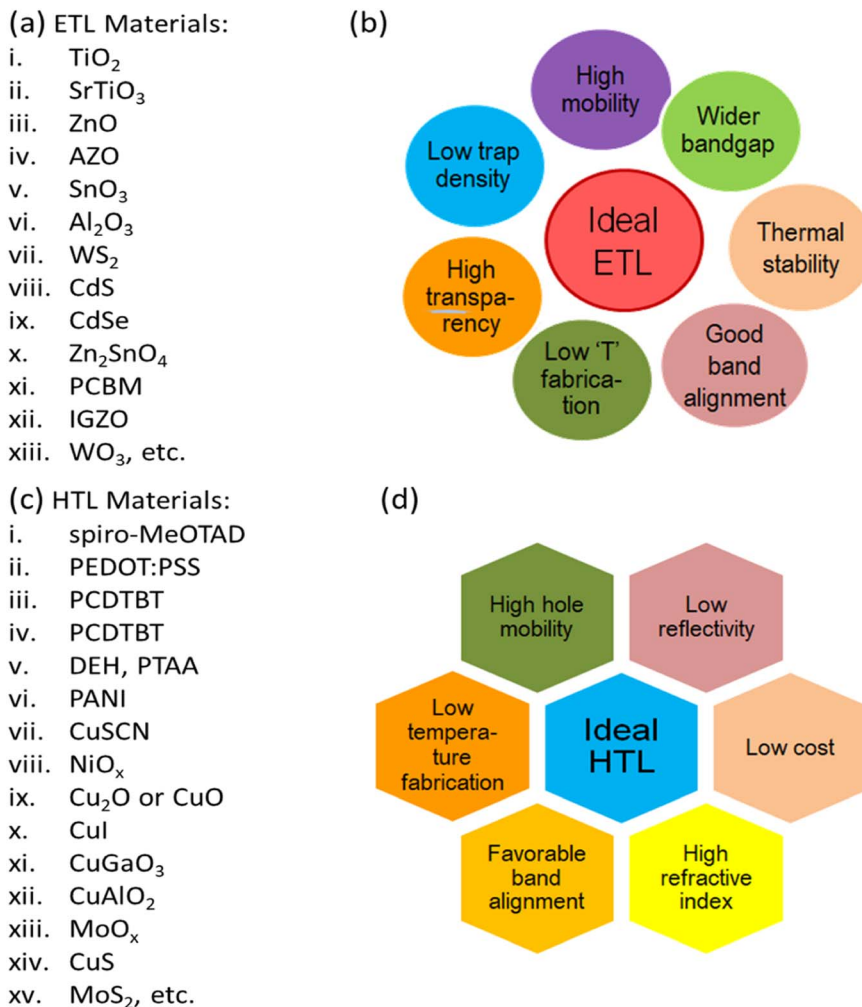


Fig. 2 ETL and HTL materials used for PSCs (a) different ETL materials for PSCs, (b) properties of an ideal ETL, (c) different HTL materials for PSCs, and (d) properties of an ideal HTL.

Seok's group has improved the PCE to 12.3%.⁵⁹ However, Snaith *et al.* used Al₂O₃ thin film \approx 80 nm instead of TiO₂ to fabricate a regular junction thin-film solar cell with the PCE of 12.3%.⁶⁰ For higher electron mobility and proper bandgap (3.7 eV) at 25 °C temperature, ZnO is found as the new alternative to the TiO₂ layer. Mahmood *et al.* have designed such PSCs with the PCE of 12% by using the electro-spraying method.⁶¹ In the end, the stable active layer remains the main focus to increase the stability of the PSC.

4.2 Planar PSCs (n-i-p or p-i-n)

Particularly, planar PSCs have two basic structures with respect to the position of the carrier transport layers; (i) regular planar; n-i-p configuration: ETL/perovskite/HTL and (ii) inverted planar; p-i-n configuration: HTL/perovskite/ETL.^{59,62} The structures including the band diagram are schematically shown in Fig. 3(b) n-i-p planar and Fig. 3(c) p-i-n planar PSCs. The energy band diagram of PSC with structure of n-i-p and p-i-n are shown in Fig. 3(d) and (e) respectively.

Easy processing, low cost, and low-temperature process are some unique features of planar PSCs.⁶¹ The normal planar structure is similar to the mesoporous PSCs but it does not use mesoporous materials.⁶³ The device performance of PPSC (perovskite piezo-phototronic solar cell) depends on each layer including the properties of HTL and ETL.⁶⁴ Many strategies have already been reported that the high performance of planar p-i-n PSCs is very much influenced by crystalline regulation and band to band matching in between the different active layers,⁶⁵ modification of perovskite materials *via* elemental variation,⁶⁶ control of geomorphology,⁶⁷ and carriers transport layers' modification.⁶⁸ To regulate the energy level, the perovskite layer is usually sandwiched by PCBM as ETL and PEDOT:PSS as HTL. Yu *et al.* reported a 31% improvement in device performance, with an average PCE of 14.61%.⁶⁹ Also, the interfacial modification method showed an efficiency rate of 16% and also guaranteed long-term stability. Nearly 19.5% efficiency was found when the planar device was developed with SnO₂ as an electron selective layer *via* the atomic layer deposition (ALD) process. SnO₂ is useful for its well-aligned conduction band in

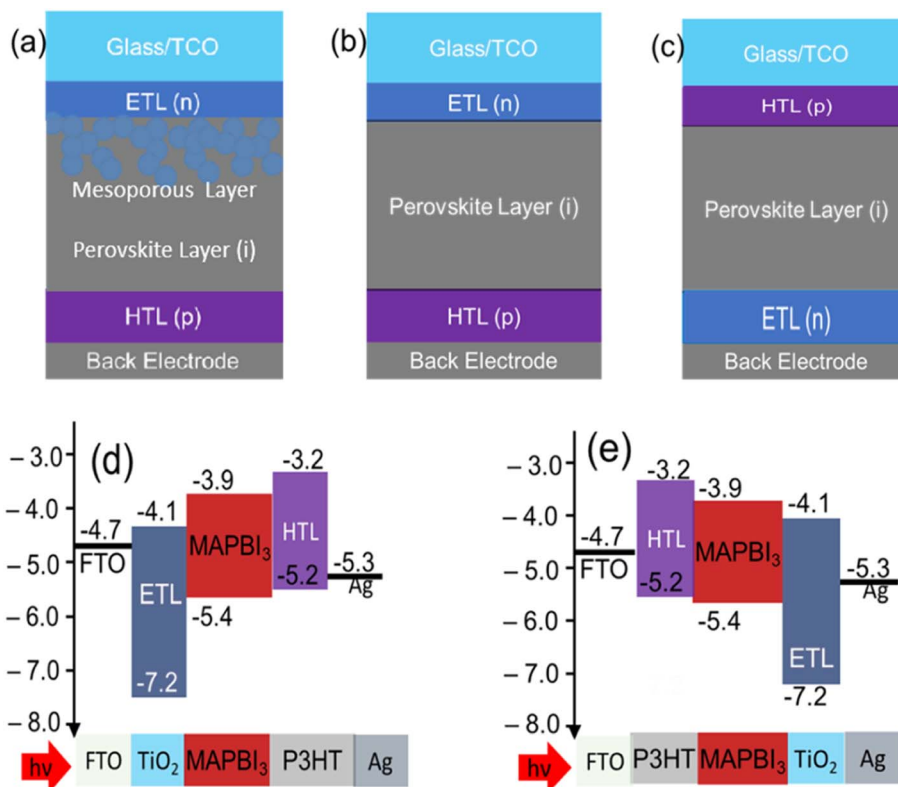


Fig. 3 Device structures of PSCs (a) n-i-p mesoscopic, (b) n-i-p planar and (c) p-i-n planar PSCs and energy band diagram of PSC with structure of (d) n-i-p and (e) p-i-n.

planar configuration.⁷⁰ For large-scale manufacturing low temperature is suitable, as claimed by Anaraki *et al.*⁷¹ Luo *et al.*⁷² came out with 21.11% efficiency and also stabilized power output of 20.83%. For planar PSCs, high efficiency is yet to be found and relentless efforts are in process.

On the other hand, high stability, easy fabrication method, and negligible hysteresis are some features of inverted structure PSC devices.⁷³ For flexible and high-performance photovoltaic devices, inverted PSCs are preferable.⁷¹ PEDOT:PSS has been widely used as HTL for inverted solar cells because its conductivity and transparency in the visible range are good enough⁷² as well as it shows unique hydrophilic and water absorbing properties.⁷⁴ Most of the high-efficiency inverted PSCs are built with HTL (PEDOT:PSS) and ETL (PCBM, ICBA, C₆₀-SAM) organic semiconductors.^{75–77} Particularly, the concept of organic photovoltaics has inspired the fabrication of the first inverted planar PSCs which used PEDOT:PSS and PCBM as carrier-transporting material. Comparing between normal structure (FTO/TiO₂/MAPbI₃/PTAA/Au) with the inverted structure (ITO/PEDOT:MAPbI₃/Au/PCBM), Heo *et al.*⁷⁸ found that the normal structure had less efficiency than the inverted structure. It has been found that the modified PEDOT:PSS HTL resulted in a 15.7% increase in PCE, 1.06 V increase in V_{oc} , and also shows better long-term stability.⁷⁹ Wang *et al.*⁸⁰ doped PEDOT:PSS solution with sodium chloride (NaCl) and have fabricated highly efficient PSCs with high FF and V_{oc} yields. NaCl affects the nucleation and development of PEDOT:PSS as well as the

electrical characteristics of PEDOT:PSS. At the optimal NaCl doping dose of 5 mg mL⁻¹, a high FF (80%) and a high V_{oc} (1.08 eV) have been achieved, as a result, PCE reached 18.2% for the MAPbI_{3-x}Cl_x based PSCs and DA-PADOT:PSS based PSC shows long term performance compared to PEDOT:PSS in un-encapsulated circumstances according to Huang *et al.*⁸¹ J_{sc} and PCE both kept 89.2% and 85.4% of their initial values respectively. With a PCE of 14.82%, Yang *et al.*⁸² demonstrated a high-performance planar heterojunction PSC. By putting the Ca between the PCBM and electrode, Chiang *et al.*⁸³ attained the best PCE of 16.31%. By developing the inverted device with structure ITO/PEDOT:PSS/MAPbI₃/PCBM/Au; Li *et al.* were able to reduce hysteresis that is less than the planar MAPbI₃ perovskite hybrid solar cells with 18.1% of PCE.⁸¹

Particularly, the highest PCE of 23.56% in planar PSCs is achieved with spiro-OMeTAD as HTL instead of PEDOT:PSS.⁸⁴ Also, another popular organic HTL is P₃HT where the highest PCE of 23.3% has been reported elsewhere.⁸⁵ In contrast, several low-cost inorganic HTLs were also proposed and implemented for enhancing the stability of PSCs, among them, some of HTMs are CuSCN,⁸⁶ NiO_x,⁸⁷ Cu₂O or CuO,^{87,88} CuI,⁸⁹ CuGaO₃ (ref. 90) and CuAlO₂,⁹¹ MoO_x,⁹² CuS,⁹³ MoS₂ (ref. 94) and polymer electrolyte.^{69,95} The above-mentioned HTMs have shown potential as they offer suitable properties for application in PSCs including the suitable band to band alignment with the perovskite layer, low resistivity, and low-cost solution-process ability. The highest PCE of 21.66% has been reported for NiO_x HTM where cell



PCE retains 90% over 1200 h of exposure in the normal ambient.⁶⁹ In the case of inorganic HTM, increased demand will dramatically reduce the cost of any large-scale manufacturing, but organic HTM is likely to remain costly due to the preparation methods and high purity needed for solar cell applications. This is the primary reason why researchers have concentrated their efforts on the development of an inorganic HTM. Consecutively, the quest for the perfect HTM is a great topic yet. There is a lot of literature on various HTMs, but only a few of them show promise in terms of improving the overall efficiency and stability of the PSCs. Several approaches have been evolved to utilize inorganic p-type semiconductor materials, such as NiO_x, CuO_x, *etc.* focusing on developing non-hygroscopic and highly conductive HTMs. Also, carbon-based materials including graphene, carbon black, graphite powder, carbon nanotube (CNT), activated carbon, *etc.* have been used in the case of HTM-free PSC.^{96,97} Composite and/or doped graphene (GR) also provides several advantages including high optical transmittance, ease of work-function management, and high chemical stability.⁹⁸ When it comes to device stability, carbon derivatives like graphene,⁹⁹ graphene oxide,¹⁰⁰ and reduced graphene oxides¹⁰⁰ are very attractive. Kim *et al.*⁷⁸ used GR doped with gold(III) chloride (AuCl₃) as a protective layer between ITO and PEDOT:PSS for improving the efficiency and endurance of PSCs. For low temperature processed inverted planar PSCs, Chowdhury *et al.*¹⁰¹ employed reduced graphene oxide (rGO)/copper(I) thiocyanate (CuSCN) as an efficient bilayer HTL and up to 14.28% of PCE has been attained with 100 hours of light soaking stability. Instead of PEDOT:PSS, Yeo *et al.*¹⁰² proposed fluorinated reduced graphene oxide (MFGO) for utilizing as an alternative HTL. In planar inverted MAPbI₃ PSCs, Zhou *et al.*¹⁰³ recommended using a bilayer consisting of rGO and PTAA as the HTL. In particular, current approaches to HTMs are low cost, high mobility, low absorption in the visible region, ease of synthesis, and good chemical stability that could ensure high efficiency and stable PSCs. Here, we are summarizing different types of inorganic HTMs which have been employed in the fabrication of PSCs focusing on their impact on device efficiency and stability.

Aside from that, fullerene-based ETLs are the most common inverted PSCs due to their simple device architecture, low-temperature preparation technique, and minimum hysteresis activity.¹⁰⁴ The PFN-2TNDI has also been introduced as a replacement for PCBM as the ETL in inverted PSCs.¹⁰⁵ In addition, devices based on the PFN-2TNDI increased efficiency by 16.7% and demonstrated long-term stability. Zhang *et al.* designed and synthesized a novel NDI-based polymeric ETL to replace PCBM in an inverted PSC.¹⁰⁵ In the realm of polymeric ETLs, the highest photovoltaic performance was attained with a PCE of 17% and negligible hysteresis. This method improves the light-induced and long-term stability of these devices in ambient circumstances. Carbon nanoparticles, which have been widely employed in n-i-p PSCs, are emerging as feasible options for metallic electrodes due to their inexpensive cost, excellent electrical characteristics, and amazing stability.¹⁰⁴ Carbon materials have the advantages of copious supplies, excellent electrochemical stability, and hole extraction that

metal electrodes do not have.¹⁰⁴ As a result of the absence of the hole transport layer, the production process of carbon-based structures is reduced. Furthermore, the hydrophobicity of the carbon material structure can considerably improve the stability of the solar cells.

4.3 HTL free PSC

Currently, high-performance PSCs typically include a perovskite active layer sandwiched between an ETL and HTL.^{85,106} Despite its numerous advantages, the HTL/ETL may have significant drawbacks. For starters, each extra layer makes the fabrication process more difficult and increases the cost.¹⁰⁷ Furthermore, some metal oxide HTL or ETL (such as TiO₂, NiO_x) require high-temperature sintering, which is incompatible with flexible substrates and consumes a lot of energy. Moreover, these layers may have hydrophilic nature and/or photocatalytic activity which leads to the quick degradation of PSCs.¹⁰⁸ Finally, harmful organic solvents are frequently required in the HTL or ETL deposition process, which results in significant contamination during the production process. Many researchers have attempted to design novel charge-transport materials to avoid these detrimental consequences.¹⁰⁹ Moreover, HTL free PSCs have also been investigated by numerous researchers as an alternative approach as discussed hereafter. The PCE of the first HTL-free PSC was 5.5% which confirmed that perovskite can act as an effective hole transporter in this study. Snaith *et al.*¹¹⁰ substituted mesoporous TiO₂ with insulant Al₂O₃ later that year and reported PCE of over 10%, indicating that perovskite could also successfully transmit electrons. Using ultrafast spectroscopy in 2013, perovskite was confirmed to be an ambipolar semiconductor with a long charge carrier diffusion length.¹¹¹ All of these groundbreaking discoveries lay the groundwork for future PSC device architectural simplification. The photovoltaic performance of the HTL-free PSCs is summarized in Table 1.

The HTL-free design is a unique category in the history of PSC development, exhibiting good stability. Lowering the cost of production and streamlining the process would make the devices more competitive, which is crucial for commercialization. In this regard, inverted hole-transport-layer-free (HTL-free) PSCs developed and have garnered a lot of interest. Inverted HTL-free PSC efficiency has currently topped 20%, and after 1000 hours of nonstop illumination, 90% of the initial efficiency may still be maintained.¹¹² Also, HTL-free devices can significantly reduce the complexity of processing and the fabrication costs, which can make them suitable for large-scale fabrication.^{113,114} This year, Zhou *et al.* reported HTL free PSC with highest PCE of 22%.¹¹⁵ The higher PCE found by fabricating high quality and pin hole free perovskite with bigger average grain size (above 1 μm) *via* synergistic doping Cu(thiourea)Cl (Cu(Tu)Cl) and thiosemicarbazide into the perovskite precursor solution. Additionally, they noted that the effective passivation of defects at grain boundaries and point defects in the perovskite film may be achieved by the synergistic doping of Cu(Tu)Cl and TSC. This helps to facilitate hole transit and lessen charge carrier recombination. The device also showed long term operational stability as shown in Fig. 4. This finding suggested



Table 1 Summarized photovoltaic performance of the HTL-free PSCs

| Year of publication | Structure | PCE (%) | Stability | Stability test parameters | Ref. |
|---------------------------|--|---------|---|--|------|
| Normal structure | | | | | |
| 2012 | FTO/c-TiO ₂ /TiO ₂ nanosheet/MAPbI ₃ /Au | 5.5 | — | — | 117 |
| 2013 | FTO/c-TiO ₂ /m-TiO ₂ /MAPbI ₃ /Au | 8.0 | — | — | 118 |
| 2014 | FTO/c-TiO ₂ /m-TiO ₂ /MAPbI ₃ /Au | 10.85 | — | — | 119 |
| 2015 | FTO/c-TiO ₂ /m-TiO ₂ /MAPbI ₃ /C/Al | 13.53 | — | — | 120 |
| 2016 | FTO/c-TiO ₂ /CsPbIBr ₂ /Au | 4.7 | — | — | 121 |
| 2018 | FTO/c-TiO ₂ /m-TiO ₂ /MAPbI _{3-x} Cl _x /C | 14.3 | PCE of around 97.7% retained | 210 d, 20 °C, RH (40–70%) | 122 |
| 2018 | FTO/c-TiO ₂ /m-TiO ₂ /MAPbI ₃ -SWCNT/SWCNT-C | 15.73 | PCE of around 100% retained | 90 d, dark, (i) RH [65 ± 5%], 25 ± 5 °C (ii) RH (25 ± 5%), 75 ± 5 °C | 123 |
| 2018 | TO/c-TiO ₂ /MAPbI ₃ /C | 13.52 | PCE of around 100% retained | 1200 s continuous light (1 sun, 1.5 AM) | 124 |
| 2019 | FTO/c-TiO ₂ /m-TiO ₂ /PbTiO ₃ /MAPbI ₃ /CNT | 16.37 | (i) PCE of around 95% retained (ii) PCE of around 70% retained | (i) 70 d, dark, RH 20%, 25 °C (ii) 40 d, dark, RH70%, 25 °C | 125 |
| 2019 | FTO/c-TiO ₂ /m-TiO ₂ /MAPbI ₃ /MAPbI ₃ Br _{3-x} /C | 16.3 | PCE of around 85% retained | Few days, RH 30%, 23 °C | 126 |
| Inverted structure | | | | | |
| 2015 | ITO/MAPbI ₃ /PC ₆₁ BM/bis-C60/Ag | 11.02 | — | — | 127 |
| 2015 | TO/MAPbI ₃ /C ₆₀ /BCP/Ag | 16 | PCE of around 80% retained | 3 d, glove box ambient (H ₂ O <0.01 ppm, O ₂ <50.00 ppm) | 128 |
| 2016 | ITO glass/MAPbI ₃ /PC ₆₁ BM/Al | 11.7 | PCE of around 99% lost | 300 m, RH 30%, 20 °C | 129 |
| 2017 | ITO/MAPbI ₃ (Cu(Tu))/C ₆₀ /BCP/Ag | 19.9 | (i) PCE of around 89% retained (ii) PCE of around 50% retained | (i) 55 d, dark (ii) 14 h, illumination and working condition | 130 |
| 2018 | ITO/MAPbI ₃ -F4TCNQ/C ₆₀ /BCP/Cu | 20.2 | PCE of around 92% retained | 500 h, ambient condition, RH 20%, 25 °C | 107 |
| 2019 | ITO/TAPC-ML/MAPbI _{3-x} Cl _x /C ₆₀ /BCP/Ag | 19.4 | PCE of around 100% retained | 600 s, continuous light, RH 40% | 131 |
| 2022 | ITO/Cs _{0.03} (FA _{0.92} MA _{0.08}) ₉₅ Pb(I _{0.92} Br _{0.08}) ₃ /ETL/BCP/Cu | 22 | PCE of around 90% retained | 1000 h, contentious white light, N ₂ ambient | 115 |

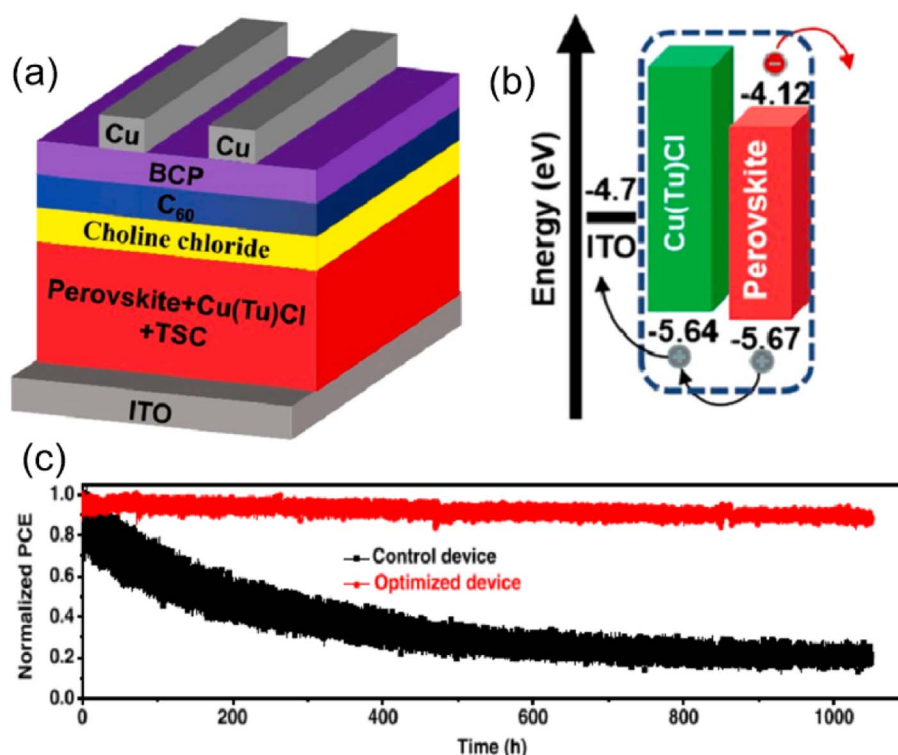


Fig. 4 (a) Schematic diagram (b) corresponding band diagram of HTL free PSC, and (c) operational stability of the encapsulated device under MPP tracking and constant light illumination from a white LED lamp (100 mW cm^{-2}) operating at room temperature in a test box filled with N_2 , (reproduced from ref. 115 with permission from Elsevier, copyright 2022).

that in the case of HTL free PSC, p-type doping in perovskites is required for fabricating operationally stable devices with high PCE. However, the carrier recombination at the perovskite/electrode interface may increase and electron blocking is difficult. Besides, a comparison study of planar and mesoporous PSCs with printed carbon electrodes has been published by Chen *et al.*¹¹⁶ Mesoporous TiO_2 was discovered to have a better PCE because it allows for effective electron extraction from the perovskite absorber, which prevents substantial carrier recombination in the hole transport layer free device caused by hole buildup. In short, organic HTLs like spiro-OMeTAD, PTAA, and others are used by the majority of high-efficiency PSCs. Because these molecules have well-aligned energy levels with perovskites, energy loss during carrier transport is considerably decreased. However, most organic HTLs are thermally unstable, and ionic additives are frequently added to improve their conductivity, again worsening the device stability.¹¹² On the other hand, inorganic HTLs and HTL-free techniques have been shown to improve the stability of PSCs, conversely, their low device efficiency is a key barrier to their commercialization.

4.4 ETL free PSC

ETLs are particularly useful for extracting electrons and blocking holes from PSCs' active layer. They're n-type semiconductors with the smallest number of vacant molecular orbitals and the highest electron mobility. Fullerene derivatives like PC_{61}BM and C_{60} , as well as inorganic metal oxides like TiO_2 , SnO_2 , and

ZnO , are the most often utilized ETLs. Finding the best-suited ETL for highly stable PSC remains a challenge. As it was mentioned earlier that organic materials are prone to the ambient condition, especially humidity and light that lead to the PSCs' instability. Metal oxide films appear to improve the stability of PSCs, but their deposition necessitates high-temperature sintering or a complicated synthesis method, which may have an impact on the underlying layers and encourage perovskites degradation.

Particularly, there is an unfavorable chemical interaction between ZnO and metal halide perovskites has been reported, which causes the perovskite to degrade rapidly.¹³² Moreover, defects in the SnO_2 layer can vary greatly depending on the deposition technique, which affects the J - V characteristic and the performance of PSCs. Ionic charge accumulation and non-radiative recombination can be caused by defects at the SnO_2 /perovskite interface, which have an impact on the hysteresis effect and device performance.¹³³ Additionally, SnO_2 's terminal state may have an impact on how perovskite absorbers develop.¹³⁴ Besides, the use of a high-temperature deposition process of ETL may increase the manufacturing cost and energy consumption. Particularly, if we can omit ETL from the structure, we can fabricate PSCs with a simpler procedure and improved stability. As a result, ETL-free PSCs with comparable performance to their ETL counterparts are regarded to be commercially viable. However, in comparison to conventional ETL-embedded devices, performance and stability of ETL-free



devices are much lower. Poor-quality perovskite layers with low charge mobility, inadequate surface coverage and uniformity, high defect densities, low built-in potential, short diffusion lengths, and misaligned energy levels between perovskite and conductive substrates are the main factors preventing further improvement of the cell efficiency.¹³⁵ The photovoltaic performance of the ETL-free PSCs is summarized in Table 2.

It should be noted that due to the absence of ETL, the electron extraction behaviors of ETL-free PSCs differ from those of typical PSCs with n-i-p or p-i-n structure. Some believe that electron extraction in ETL-free PSCs is driven by the built-in electric field at the TCO/perovskite interface, while others believe that charge accumulation in the perovskite layer is the driving element for charge transfer across the TCO/perovskite interface.¹³⁶ The ETL-free PSC has been reported early in 2014 (ref. 137) and found that the ETL-free PSCs show significantly lower PCE than those of PSCs with ETL. Numerous efforts have been taken in recent years to improve the performance of ETL-free PSCs, but their stability has not been thoroughly investigated. Particularly, the operating mechanism of ETL-free PSCs has been thoroughly investigated in seven years of development, and device performance has greatly increased. The highest PCE achieved in ETL-free PSCs is 20.55% so far,¹⁰⁷ which is similar to the PCE of PSCs with ETL. ETL-free PSCs are projected to have a bright future and substantial research initiative has been conducted toward large-scale manufacturing, flexible devices, and long-term stability. Particularly, the barrier is the energy level mismatch between perovskite and conducting oxide (ITO) and a weak built-in electric field, which leads to poor charge extraction and substantial charge recombination that occurred at the TCO/perovskite interface. These obstacles can be overcome by increasing the carrier lifetime in perovskite that offered enough time for sufficient electron extraction, and/or by modifying interfacial band alignment by employing an additional layer. Excess PbI₂ has been discovered to significantly increase the carrier lifetimes and PL quenching rate of perovskite (MAPbI₃) films, hence increasing the device performance. By using thick perovskite films (about 700 nm) and analyzing the microsecond carrier lifetime of perovskite films, Han *et al.* achieved a high PCE of 18.1% for HTL-free PSC with negligible hysteresis.⁷⁸ Thus, the built-in electric field was found to be the driving force of electron extraction at the TCO/perovskite interface and proposed a practical technique for improving the electron extraction at the interfaces. Actually, a high amount of electron generation in perovskite raises the electron quasi-Fermi level of perovskite films, as opposed to the hole quasi-level in HTLs which influences the electron extraction. However, the mechanism by which ETL-free PSCs function is not clear yet, demanding further research and *in situ* characterization.

4.5 Tandem PSCs

The tandem structure has been a stride forward in PSCs commercialization. There are additional processing steps needed to fabricate a tandem cell and are expecting improved efficiency and stability of the cell. An exhaustive review

Table 2 Summarized photovoltaic performance of the ETL-free PSCs

| Year of publication | Structure | PCE (%) | Stability | Stability test parameters | Ref. |
|---------------------|--|---------|---|---|------|
| 2014 | ITO glass/MAPbI ₃ /spiro-OMeTAD/Ag | 13.5 | — | — | 137 |
| 2015 | ITO glass/MAPbI ₃ /P ₃ HT/Ag | 14.14 | >70% of PCE retained | 500 h, RH 20%, dark | 138 |
| 2015 | FTO glass/MAPbI _{3-x} Cl _x /spiro-OMeTAD/Au | 9.95 | — | — | 139 |
| 2016 | ITO glass/MAPbI ₃ /PBDDTTT-C/MoO ₃ /Ag | 13.6 | PCE of 7% retained | 3 h, continuous light illumination (1 sun) | 140 |
| 2016 | FTO glass/MAPbI ₃ :C ₇₀ /spiro-OMeTAD/Au | 12.91 | PCE 70% retained | 300 h, ambient environment | 141 |
| 2017 | ITO glass/PEDOT:PSS/MAPbI ₃ /Ti/Au | 15.69 | No degradation | 21 d, ambient air and dark condition | 142 |
| 2017 | FTO glass/MAPbI ₃ /spiro-OMeTAD/Au | 14.3 | No significant degradation | 124 h, continuous light (AM 1.5, 1 sun) | 143 |
| 2017 | FTO glass/CsFAMA (formamidinium methylammonium)/spiro-OMeTAD/Au | 15.42 | — | — | 144 |
| 2018 | FTO glass/BCP/CsFAMA/spiro-OMeTAD/Ag | 19.07 | PCE retained 92.2% | 500 h, continuous light (AM 1.5, 1 sun) | 145 |
| 2018 | FTO glass/MAPbI ₃ /spiro-OMeTAD/Au | 12.60 | PCE dropped by 4.0% | 374 h, stored in the ambient environment | 146 |
| 2018 | FTO glass/MAPbI _{3-x} Sb _{2y} I _{3-2y} Cl _x /spiro-OMeTAD/Ag | 12.62 | PCE retained about 70% | 148 h, RH 20%, room temperature | 147 |
| 2019 | FTO glass/TMAH/FAMA/spiro-OMeTAD/Au | 20.1 | PCE retained about 83% | 500 h, RH 25%, 30 °C | 148 |
| 2019 | FTO glass/Maze-like MAPbI ₃ /spiro-OMeTAD/Au | 18.5 | — | — | 149 |
| 2019 | FTO glass/MAPbI ₃ /spiro-OMeTAD/CANPs/Au | 18.89 | (i) PCE retained about 70% (ii) PCE retained about 80% | (i) 25 °C, 35% RH (ii) 540 m, continuous light (AM 1.5, 1 sun) | 150 |
| 2020 | ITO glass/MAAc/MAPbI ₃ /spiro-OMeTAD/Au | 21.08 | PCE retained about 86% | 400 h, continuous light (AM 1.5, 1 sun) | 151 |
| 2021 | TETA-GR/BCP/MAPbI ₃ :GQDs/PTAA/Au | 15.72 | PCE retained about 83% | 500 h, ambient environment | 152 |
| 2021 | ITO/MSAPBS/(FAPbI ₃) _{0.85} (MAPbBr ₃) _{0.15} /spiro-OMeTAD/Au | 20.55 | — | — | 153 |

©
RSC

cluded that the separation layer between the two cells should be stable and that the best choice for reducing recombination in the cell/intermediate layer interface is a solution-processed thin layer based on Ag nanostructure. In early 2013, Heliatek revealed organic polymeric tandem solar cells with a PCE of 12%, with vacuum evaporated cells outperforming solution-processed cells.¹⁵³ The fabrication process optimization and investigation of interconnection losses have pushed up efficiency,¹⁰⁷ however, only a PCE of 13.8% has been achieved,¹³¹ and still far below the maximum projected PCE of 21% for organic tandem cells.¹⁵⁴ In addition, the perovskite/Si tandem exhibits the greatest promise of all the varieties. Inverted perovskite/silicon V-shaped tandem solar cells with a PCE of 27.6% were reported by Zheng *et al.* Beside, for monolithic PSC/Silicon tandem solar cells,¹⁵⁶ Al-Ashouri *et al.* reported a PCE of 29.15%.¹⁵⁵ However, the equivalent parameter used in the PSC/Si tandem cells is still significantly lower than that of the high-performing single junction c-Si cells. As a result, there is still more space for advancement in tandem solar cells that use bottom cells. It should be noted that the Si-based tandem cells' theoretical maximum efficiency might be raised from 29 to 42.5%.¹⁵⁷ Furthermore, as the photocurrent of monolithically integrated tandem solar cells is controlled by the two subcells' photocurrents, any mismatch in the current of top and bottom cell will result in a significant loss of power. The transparent

electrode, ETL, and HTL sheet resistances are also be crucial in figuring out the total PCE.

Particularly, tandem photovoltaics is a realistic approach for reducing thermalization losses in solar energy conversion by integrating two absorber layers into a single device with unique bandgap energies. Recently, perovskite-silicon tandem solar cells have risen to prominence as the preferred energy conversion device, with the potential to achieve ever-higher efficiencies. However, if the top and bottom cells can operate near to their theoretical limits, then only the higher PCE is possible. Tandem devices have typically been built utilizing two-terminal (2T) or four-terminal (4T) configurations as shown in Fig. 5(a) and (d).¹⁵⁸ In 2T configuration, two devices are connected in series, and the connection requires current matching which limits the device performance, whereas the standard 4T configuration needs a minimum of three transparent electrical contacts, which may increase unavoidable parasitic absorption and reduces total collected power. Electronically and optically linking the top and bottom cells in 2T arrangements can help reduce non-radiative recombination loss and reflections between the devices, which are frequent in 4T tandem cells. However, even with the best design, this current matching condition in 2T tandem can only be achieved for a single optical spectrum, and under diffuse light conditions, major variations in the illumination spectrum can result in significant efficiency losses.¹⁵⁹ On the other hand, electronic decoupling of the two

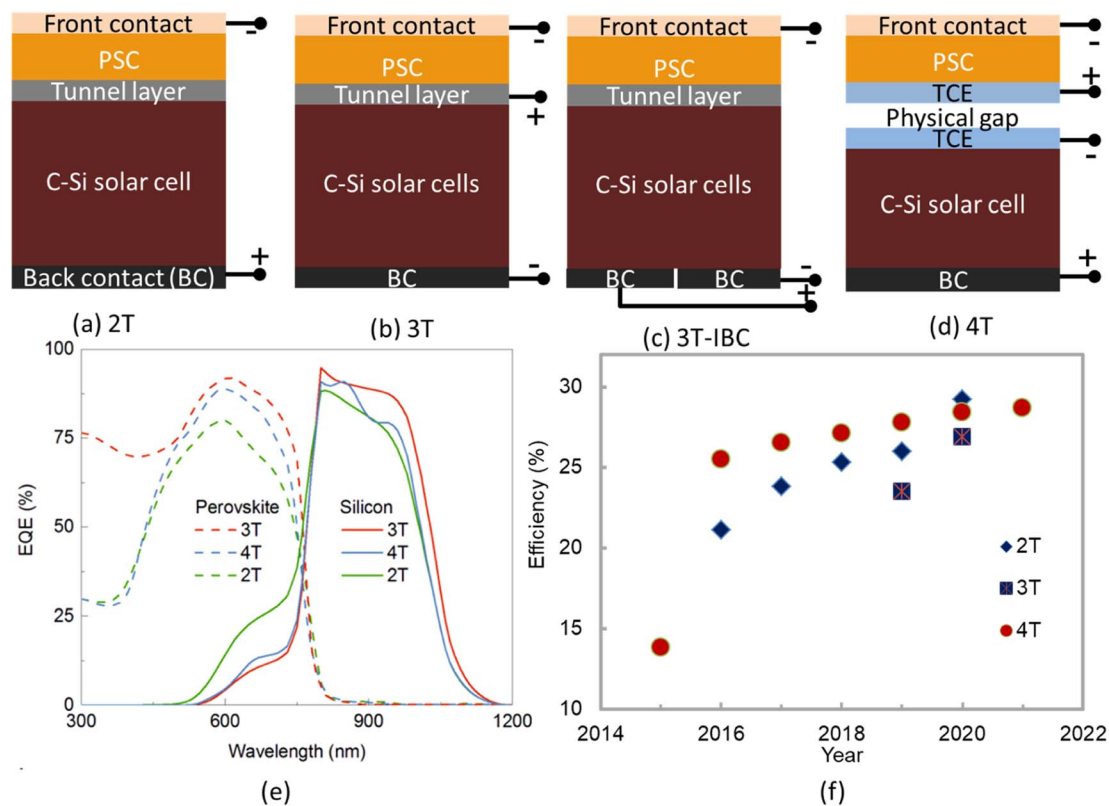


Fig. 5 (a–d) Schematic diagram of different perovskite–Si tandem solar cells, (e) EQE of perovskite and silicon tandem solar cells for 2T, 3T (IBC), and 4T configuration, and (d) highest reported efficiency by a different configuration of perovskite–Si tandem solar cells, (reproduced from ref. 158 with permission from ACS publications, copyright 2017).

cells in 4T devices reduces the need for current matching, but thick spacer layers in 4T tandem often affect the optical benefits and the additional contact contributes a 10% relative efficiency loss.¹⁶⁰ As a result, the 3-terminal (3T) arrangement has been proposed, as illustrated in Fig. 5(b) and (c), to achieve a tandem device that is optically connected but electrically decoupled, and to gain the benefits of both traditional topologies while avoiding their principal shortcomings. The EQE curves as shown in Fig. 5(e) confirm the benefits of the 3T over 2T and 4T tandem PSCs. Fig. 5(f) shows the highest PCE for different tandem configurations reported so far. The continuous improvement in PCE is observed over the year for all types of tandem devices.

All the tandem configurations have proven to be effective for higher PCE, where the key problem in achieving near the theoretical efficiency limit in tandem is to optimize the inter-connecting layers.¹⁶¹ Importantly, because of the reduced use of glass, manufacturing two-terminal tandem cells minimizes environmental consequences by up to 30% compared to two single-junction devices. Other than c-Si as the bottom cell, CIGS and CZTS bottom cells, as well as a full perovskite tandem (SnPb/Pb), have also been constructed and studied. The entire perovskite (SnPb/Pb) (tin lead/lead) structure has considered to be the most ecologically beneficial technology; however, the efficiency of the device should be near 30% and a 16 year lifetime to compete with Si technology.¹⁶² For the time being, PSC on Si based solar cells is the alternative technology that is rapidly being investigated as mentioned above, with a company (Oxford PV Ltd) that may soon be able to commercialize it.¹⁶³

4.6 Flexible PSCs

In high-efficiency flexible solar cells, ITO-coated flexible polymer substrates, such as PET and PEN, are widely employed as electrodes. Low conductivity, poorer transmittance, and poor mechanical resilience are the main limitations of ITO on flexible polymer substrates when compared to ITO-coated rigid glass substrates.¹⁶⁴ It is also well recognized that most polymer substrates can't sustain temperatures above 250 °C. As a result, all depositions and treatments must be performed at a lower temperature, resulting in lower ITO resistivity (more than 20 Ω sq^{-1}).¹⁶⁵ To compensate for the low conductivity, thicker ITO coatings are used to boost conductivity. The commercial ITO coating on PET is around 400 nm thick, but the ITO coating on glass is just 150 nm thick. Thicker ITO, on the other hand, reduces transmittance, which reduces short-circuit current density (J_{sc}) and PCE. As a result, flexible perovskite solar cells (F-PSCs) often have lower PCE than rigid perovskite devices. Mechanical bending stability is another important measure in F-PSCs. It has been reported by Seok's group that the effectiveness of PEN/ITO-based flexible PSCs was lowered after 300 bending cycles and only retains 5% of its initial efficiency. With a PCE of 12.2%, Kim *et al.*¹⁶⁶ reported an F-PSC based on identical substrates, however, after 1000 bending cycles under a 10 mm bending radius, 50% of the initial efficiency was lost. Carlo *et al.*¹⁶⁷ identified that ITO can be bent to a radius of 14 mm without cracking, however when the radius is smaller

than 14 mm, the ITO covers cracks, causing significant conductivity degradation. By sandwiching a thin Ag layer between PET substrates and ITO, Yang *et al.*¹⁶⁸ recently obtained a maximum efficiency of 18.40%. Even though the bending radius was reduced, the PCE retained 83% of its initial efficiency.¹⁶⁹ Other flexible electrodes, including conducting polymer, carbon, graphene, Ag-NWs, *etc.* could also be a better solution to improve F-PSC mechanical stability.¹⁶⁹

Long-term environmental stability is an important factor for assessing any solar cells for practical uses. However, the PSCs have yet to overcome this obstacle. The instability is caused by HTL's susceptibility to the environment and the deterioration of perovskite. Due to their low temperature and ease of manufacturing, spiro-OMeTAD, PTAA, and PEDOT:PSS has been widely employed as HTLs in F-PSCs to date. To replace the commonly used HTLs, some stable hole-transport materials such as NiO, CuI, and poly(3-hexylthiophene) (P_3HT), have been produced at low temperatures.¹⁷⁰ These HTLs have increased the stability and performance of F-PSCs. Because perovskite absorbers are extremely sensitive to dampness, oxygen, and UV light, they degrade and undergo a phase transition in flexible devices. Given the importance of industrialization's stability, encapsulation technology has emerged as a critical technique for protecting delicate cells from corrosive environments. Effective encapsulation of F-PSCs is a significant difficulty. A flexible sealing film with a low water vapour transmission rate (WVTR) and low oxygen infiltration can be utilized to cover the surface of the front active region. On the backside, flexible materials with high transmittance, low oxygen infiltration, and low WVTR must be enclosed. Metal oxide deposition techniques such as physical vapor deposition (PVD), atomic layer deposition (ALD), plasma-enhanced chemical vapor deposition (PECVD), and other techniques have been shown to be effective at sealing the backside.¹⁷¹

4.7 The development of single-crystal PSC and possibility for commercialization

Perovskite single crystals (PSC) provide some unique advantages such as lower trap densities and better transport characteristics. It has been anticipated that perovskite single-crystal solar cells might achieve a power conversion efficiency of 25% with these properties.¹⁷² By using the cavitation-triggered asymmetrical crystallization method, a single-crystal film with thicknesses of tens of micrometers and lateral dimensions varying from hundreds of micrometers to 3 mm. The PSCSC with the thinnest film (1 μm) produced the maximum efficiency of 6.53% by utilizing the structure of $\text{FTO}/\text{TiO}_2/\text{MAPbBr}_3/\text{Au}$.¹⁷³ By using the space-limited inverse temperature crystallization, thin single crystals with noticeably greater lateral sizes (6 mm \times 8 mm) and the controllable thickness of micrometers (16 μm) were produced also crystals attained 7.11% PCE when used in the $\text{FTO}/\text{TiO}_2/\text{MAPbBr}_3/\text{spiro}/\text{Au}$ structure.¹⁷⁴ Single crystal perovskite solar cells have grown and improved in efficiency significantly during the last three years. Single crystal perovskite solar cells provide an ideal model system for future research into the working principles relating to perovskite surface and



grain boundaries, in addition to having higher efficiency and better stability. It is anticipated that single crystal perovskite solar cells would soon outperform polycrystalline solar cells in terms of efficiency and stability due to their better optoelectronic features and stability. Therefore, its commercial application is expanding globally. Also over the past few years, the fabrication process for single crystal perovskite solar cells has

made significant progress. Basically the fabrication processes for PSCs are of main two types such as solution based process and vapor based process as shown in Fig. 6.

Some of the examples of solution based and vapor based fabrication processes are shown schematically in the Fig. 7 and 8. The readers are suggested to follow the literature for details of the fabrication process.¹⁷⁵ Among the all processes, the spin

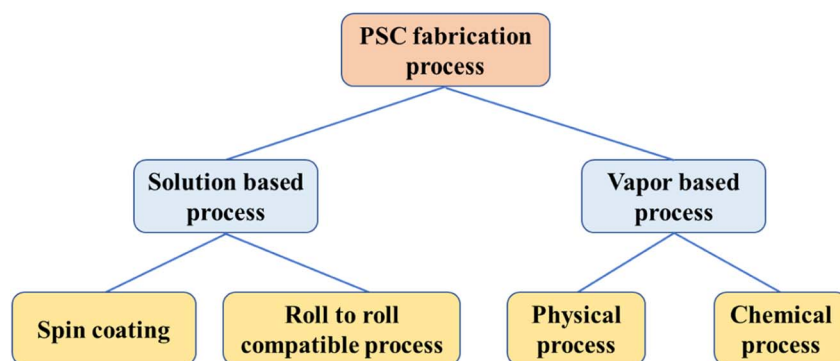


Fig. 6 Classification of PSCs fabrication process.

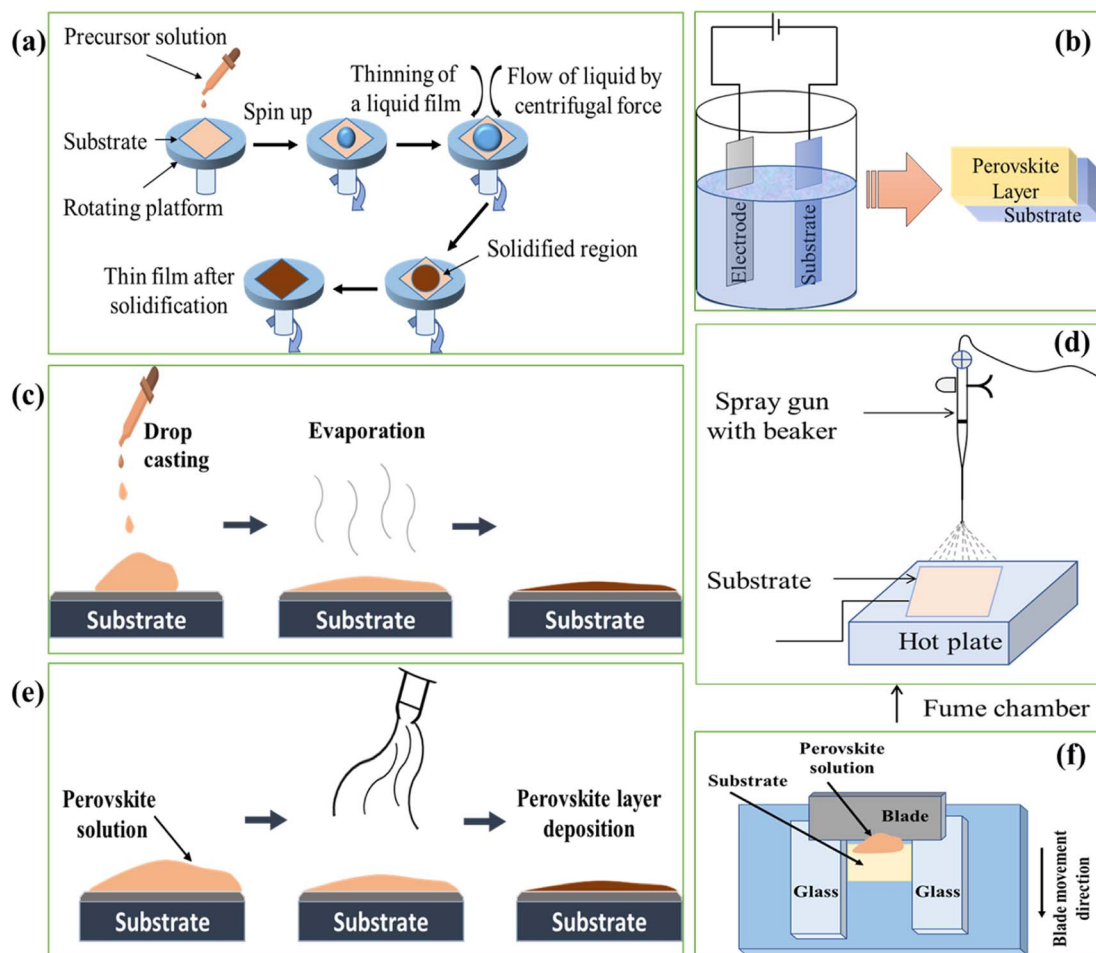


Fig. 7 Solution based PSCs fabrication processes (a) spin coating, (b) electrochemical deposition, (c) drop casting, (d) spray coating, (e) blow-drying process and (f) blade coating.

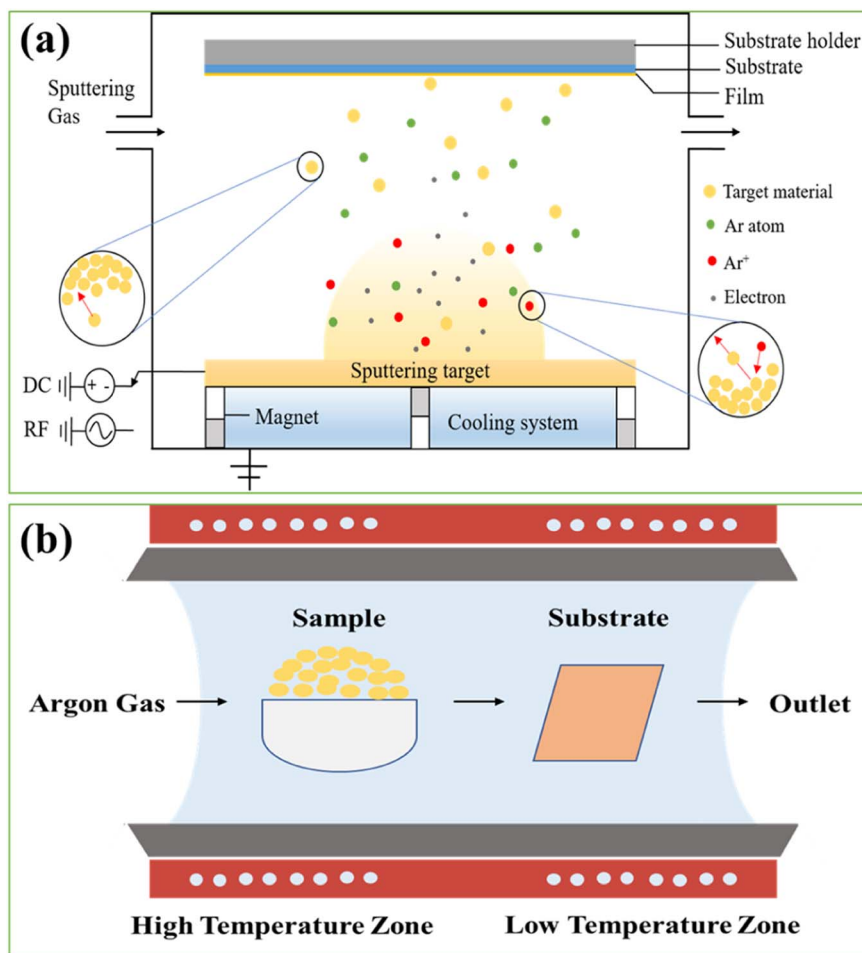


Fig. 8 Vapor based PSCs fabrication process (a) physical vapor deposition (sputtering) and (b) chemical vapor deposition.

coating process is widely used and easy process to fabricate the perovskite layer in PSCs. To achieve the practical application of single crystal perovskite solar cells, large-area production methods, specifically those satisfying industrial requirements, are more crucial.

5. Economic feasibility of perovskite devices

There are various fixed capital costs and operational costs which must be addressed carefully before creating the technology for any new kinds of solar cells. Examining the energy payback time (EPBT) of various solar cells is a cost-effective method of evaluating solar cells. EPBT may be computed using the method provided by Bhandari *et al.*¹⁷⁶

where, ϵ is the light energy to electrical energy conversion factor (often 0.35), I denoted total incident solar insolation on a unit surface per year, η is the average PCE of the modules, and PR denoted the performance ratio of the system. A PV system's PR over time is calculated as energy measured (kW h)/(irradiance (kW h m⁻²) on the panel \times active area of PV module (m²) \times PV module efficiency). Another method to analyze the efficacy of solar cells is to calculate the energy return on investment (EROI),¹⁷⁶ which is a function of EPBT and lifespan, as indicated:

$$\text{EROI} = \frac{\text{Lifetime (years)}}{\text{EPBT (year)}} \quad (2)$$

The EROI is currently developed as a 3 for any feasible solar cell technology. Besides the cell's design, the energy used in

$$\text{EPBT (years)} = \frac{\text{Embedded primary energy (MJ m}^{-2}\text{)}}{\text{Annual primary energy produced by the system (MJ per m}^2\text{ per year)}} = \frac{WI}{I \times \eta \times \text{PR}/\epsilon} \quad (1)$$



material manufacturing has also a crucial impact on EPBT solar insolation. In the electrical power sector, silicon-based PV modules have played a part in the integrated circuits in microelectronics and nanoelectronics based on silicon complementary metal-oxide-semiconductor (CMOS). In recent years, the declining prices of PV modules have led substantially to the exponential expansion of the PV industry.¹⁷⁷ The material cost for the lead iodide perovskite absorber layer is quite inexpensive, with a module size of about US \$2 per cubic meter with perovskite layer thickness up to 400 nm.¹⁷⁸ Here perovskite is the most cost-effective component, whereas the cost of transparent conductive substrates (FTO or ITO) with low sheet resistance (10 Ω per square meters) is around \$10 per square meter. The market share of thin-film PV modules is expected to shrink from 8% in 2014 to 7% in 2015, down from 15% in 2010.¹⁷⁹ On the other hand, Pb is poisonous; therefore, the environmental impact of lead PSCs should be investigated before industrialization.¹⁸⁰ Despite the fact that Pb based PSCs are more stable and well-performing, they can however significantly harm human health by polluting the environment. Organic and inorganic lead salts are both very soluble in water, making them possibly bioactive, that is, accessible to plants and thus other living beings.¹⁸¹ The European Union's hazardous substance limitation strictly controls the use of Pb in industry. Costs have dropped dramatically throughout the world, and it is anticipated that they will reduce by 66% by 2040.¹⁸² These

estimates are based on silicon-based solar cells, even though PSCs are widely recognized to be low-cost. A solar cell's life cycle was separated into four parts: module manufacture, module functioning, raw materials, and disposal.¹⁸³ Lifecycles are more significant when considering the commercialization and real-world applications of PSCs. As per our competitive and comparative analysis of high and medium PCE, the levelized cost of electricity (LCOE) of perovskite PV must reach \$0.055 per kW per h to compete with the dominant c-Si PV (PCE of 21%). Thus, we propose that a lifespan of 15 years is the standard for perovskite PV (with a PCE of 19% and a minimum module size of 100 cm²), which is a big step from the present status.¹⁸⁴ Unfortunately, lengthy stability studies are still restricted.² According to a separate report, the analysis discovered that, while the cost of active layers and rear electrodes would be reduced to null, the PCE of 18% with a 20 years lifespan would be essential for the PSC module to meet the \$0.09 per kW per h target.

6. Future prospects

One of the main aspects of the commercialization of PSCs is stability among the others such as high efficiency, easy fabrication and low cost. However, the stability data provided by various researchers can't be fairly compared because different experiment uses different testing conditions, such as

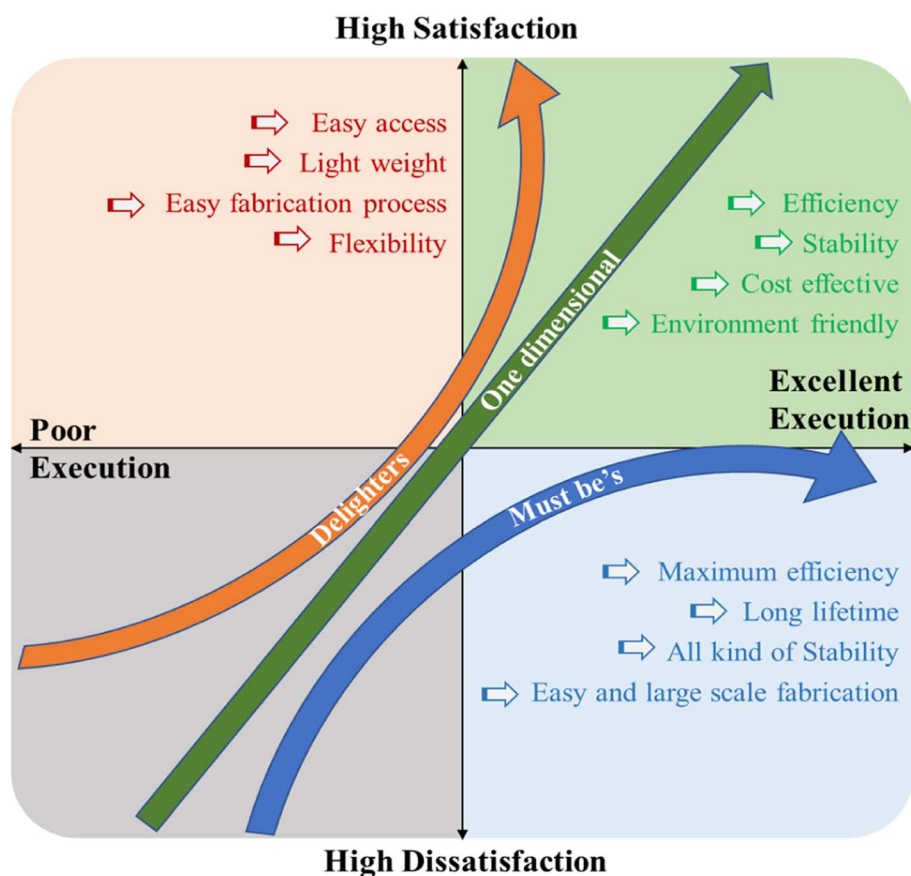


Fig. 9 Keno model for proposal of successfully commercialization of PSCs.

humidity, temperature, and encapsulation technique. Particularly, PCE is a well-defined parameter that can be validated according to standards, whereas stability-related characteristics like lifetime and deterioration rates cannot. Thus, it is crucial need to standardize the required test condition for stability testing of PSCs focusing on mechanical stability, thermal stability, device hysteresis, and stability under exposure to light, moisture, and oxygen for each fabrication technique. It should be noted that inorganic solar cell stability tests (ISOS) have approved techniques; however, they are rarely employed in the investigation of PSCs stability. Furthermore, R&D target should be set for advancement and successfully commercialization of PSCs to cope the current market demand. The Keno model imposed in Fig. 9 is a helpful tool to understand the prioritization of the features of PSCs for successfully commercialization.¹⁷⁵

The Kano model stands out in particular for its strict focus on customer perception; existing and/or prospective new product features are ranked according to the potential level of customer pleasure they may offer. The figure indicates such categorized PSCs properties that are necessary for commercialization in the current solar cell market. For market penetration, there needs to be strong research activities in these areas. The “one-dimensional” specifications have a linear connection to the quality and value of the product whereas “must be’s” are the essential requirements for the technology as well as the bare necessities for market access.

7. Conclusion and recommendation

The rapid development of PSCs in recent times is governed by the excellent and tuneable optoelectronic properties of materials which have been revealed by decades of research in the PV field. Recent findings suggest that efficiency or cost are no longer the primary concerns for PSCs, however, the short operational lifetime under normal environmental conditions is a great challenge towards commercialization. Particularly, the soft and ionic nature of perovskite materials makes it more challenging to acquire the long-time stability of PSCs in the commercialization of perovskite PV technology or to generate operationally stable PSCs. Thus, the stability of PSCs must be proven in the laboratory before their scale-up production. It should be mentioned that the stability of PSCs has recently been improved from a few minutes to thousands of hours, but this is still insufficient for practical implementation and the stability of PSCs should extend more than 10 years for commercialization. Several aspects such as modification of the structural design, use of different charge and electron transport materials including different metal-oxide films, different hole transport materials which have hydrophobic nature, modification in the electrode material preparation and encapsulation procedures, have been considered by the various researchers for systematic engineering of perovskites to improve their stability. In this review, we critically analyzed the advancement of various manufacturing techniques and structural variations of PSCs, emphasizing the degradation and stability difficulties that exist. It should be noted that a variety of degradation mechanisms

have been reported in the literature that provides a basic understanding and awareness for the augmentation of stability. It has been observed that the current modification in perovskite materials, device structure, and/or interface material is not enough for achieving higher stability as well as efficiency, and we recommend developing new materials and designs that may play a great role to overcome the aforementioned issues in the perovskite PV field.

Moreover, it should be mentioned that the HTL and/or ETL-free solar cells cannot compete with the HTL and ETL containing regular structure which generally shows higher efficiency. Similarly, lead-free solar cells clearly cannot compete with lead-containing alternatives. However, from the reported work, it is evident that HTL and/or ETL-free PSCs show lower PCE, but higher stability than HTL and ETL-containing PSCs. Also, it should be mentioned that most of the higher efficiency PSCs are used spiro-OMeTAD as an HTL, however, due to the complexity of its complex manufacturing route requiring toxic solvents, it is expensive and has been identified as a significant source of environmental impacts. As a replacement for spiro-OMeTAD, inorganic materials such as metal oxides, carbon derivatives (PCBM, carbon, graphene, or carbon nanotubes), or other organic materials (P₃HT or small molecules) have been successfully incorporated as alternatives that maintain good PCEs and in some cases extending stability. In addition, the use of FTO substrates has replaced costly ITO effectively without sacrificing efficiency or stability.

Numerous low-cost fabrication processes are commonly used in PSCs, such as spin coating, doctor blade, sequential deposition, hybrid chemical vapor deposition, and alternating layer-by-layer deposition, *etc.* It is found that the most of high PCE PSCs are fabricated using spin coating. Undoubtedly spin coating is a cheap, low cost and easiest process of fabrication. However, it does not have adequate commercial viability for large size solar cell fabrication. Thus, we have to focus on the alternate process which will ease fabricating of the commercial size of solar cells. In that case, our recommendation is the doctor blade technique which could be the most suitable for low-cost and easy fabrication for high PCE and higher stability. Finally, we would like to propose two recommendations for achieving higher stability towards future commercialization of PSCs: (i) stability tests of PSCs should be conducted using the standard protocol, such as ISOS. This will allow for a more accurate comparison of materials and device architectures, as well as a clearer picture of the research path toward extended lifetime, and (ii) the modification of fabrication technique as well as device structure and materials should comply with the ease of large-scale PSC fabrication. Moreover, new materials and designs with high stability under harsh conditions are also desirable to improve the performance of PSCs. The new materials can be used in a variety of ways, from improving existing materials to building new ones.

Data availability

All data generated or analysed during this study are included in this published article.



Author contributions

Conceptualization, M. A. I.; methodology, M. A. I., T. A. C., A. B. Z. and M. S. U. I.; software, M. A. I., T. A. C., A. B. Z. and M. S. U. I.; formal analysis, M. A. I., T. A. C., A. B. Z. and M. S. U. I.; resources, M. A. I., T. A. C., A. B. Z. and M. S. U. I.; data curation, M. A. I., T. A. C., A. B. Z., M. S. Z. and M. S. U. I.; writing—original draft preparation, M. A. I., T. A. C., A. B. Z. and M. S. U. I.; writing—review and editing, M. U. K. and M. S. Z.; visualization, M. A. I., T. A. C., and A. B. Z. All authors have read and agreed to the published version of the manuscript.

Conflicts of interest

There are no conflicts to declare.

Acknowledgements

This work was supported by the Malaysian Ministry of Higher Education through the FRGS grant FRGS/1/2020/TK0/UM/02/33.

References

- 1 M. Thirugnanasambandam, S. Iniyan and R. Goic, A review of solar thermal technologies, *Renewable Sustainable Energy Rev.*, 2010, **14**, 312–322.
- 2 N. Li, X. Niu, Q. Chen and H. Zhou, Towards commercialization: the operational stability of perovskite solar cells, *Chem. Soc. Rev.*, 2020, **49**, 8235–8286.
- 3 H. Zsiborács, N. H. Baranyai, A. Vincze, L. Zentkó, Z. Birkner, K. Máté and G. Pintér, Intermittent renewable energy sources: The role of energy storage in the European power system of 2040, *Electronics*, 2019, **8**, 729.
- 4 D. King, J. Browne, R. Layard, G. O'Donnell, M. Rees, N. Stern and A. Turner, *A global Apollo programme to combat climate change*, London School of Economics and Political Science, 2015.
- 5 H. C. Fu, V. Ramalingam, H. Kim, C. H. Lin, X. Fang, H. N. Alshareef and J. H. He, MXene-contacted silicon solar cells with 11.5% efficiency, *Adv. Energy Mater.*, 2019, **9**, 1900180.
- 6 W. C. Chang, D. H. Lan, K. M. Lee, X. F. Wang and C. L. Liu, Controlled deposition and performance optimization of perovskite solar cells using ultrasonic spray-coating of photoactive layers, *ChemSusChem*, 2017, **10**, 1405–1412.
- 7 L. Huang, X. Sun, C. Li, J. Xu, R. Xu, Y. Du, J. Ni, H. Cai, J. Li and Z. Hu, UV-sintered low-temperature solution-processed SnO₂ as robust electron transport layer for efficient planar heterojunction perovskite solar cells, *ACS Appl. Mater. Interfaces*, 2017, **9**, 21909–21920.
- 8 Z. Xiao, C. Bi, Y. Shao, Q. Dong, Q. Wang, Y. Yuan, C. Wang, Y. Gao and J. Huang, Efficient, high yield perovskite photovoltaic devices grown by interdiffusion of solution-processed precursor stacking layers, *Energy Environ. Sci.*, 2014, **7**, 2619–2623.
- 9 P. Luo, Z. Liu, W. Xia, C. Yuan, J. Cheng and Y. Lu, A simple *in situ* tubular chemical vapor deposition processing of large-scale efficient perovskite solar cells and the research on their novel roll-over phenomenon in J–V curves, *J. Mater. Chem. A*, 2015, **3**, 12443–12451.
- 10 S.-G. Li, K.-J. Jiang, M.-J. Su, X.-P. Cui, J.-H. Huang, Q.-Q. Zhang, X.-Q. Zhou, L.-M. Yang and Y.-L. Song, Inkjet printing of CH₃NH₃PbI₃ on a mesoscopic TiO₂ film for highly efficient perovskite solar cells, *J. Mater. Chem. A*, 2015, **3**, 9092–9097.
- 11 H. S. Kim, C. R. Lee, J. H. Im, K. B. Lee, T. Moehl, A. Marchioro and N. G. Park, Lead iodide perovskite sensitized all-solid-state submicron thin film mesoscopic solar cell with efficiency exceeding 9%, *Sci. Rep.*, 2012, **2**(1), 1–7.
- 12 M. M. Lee, J. Teuscher, T. Miyasaka, T. N. Murakami and H. J. Snaith, Efficient hybrid solar cells based on meso-superstructured organometal halide perovskites, *Science*, 2012, **338**(6107), 643–647.
- 13 T. Leijtens, R. Prasanna, K. A. Bush, G. E. Eperon, J. A. Raiford, A. Gold-Parker, E. J. Wolf, S. A. Swifter, C. C. Boyd and H.-P. Wang, Tin-lead halide perovskites with improved thermal and air stability for efficient all-perovskite tandem solar cells, *Sustainable Energy Fuels*, 2018, **2**, 2450–2459.
- 14 Y. Liu, Z. Yang, D. Cui, X. Ren, J. Sun, X. Liu, J. Zhang, Q. Wei, H. Fan and F. Yu, Two-inch-sized perovskite CH₃NH₃PbX₃ (X = Cl, Br, I) crystals: growth and characterization, *Adv. Mater.*, 2015, **27**, 5176–5183.
- 15 J. R. Poindexter, R. L. Hoyer, L. Nienhaus, R. C. Kurchin, A. E. Morishige, E. E. Looney, A. Osherov, J.-P. Correa-Baena, B. Lai and V. Bulović, High tolerance to iron contamination in lead halide perovskite solar cells, *ACS Nano*, 2017, **11**, 7101–7109.
- 16 A. Kojima, K. Teshima, Y. Shirai and T. Miyasaka, Organometal halide perovskites as visible-light sensitizers for photovoltaic cells, *J. Am. Chem. Soc.*, 2009, **131**, 6050–6051.
- 17 S. He, L. Qiu, L. K. Ono and Y. Qi, How far are we from attaining 10-year lifetime for metal halide perovskite solar cells?, *Mater. Sci. Eng., R*, 2020, **140**, 100545.
- 18 S. Akin, Hysteresis-free planar perovskite solar cells with a breakthrough efficiency of 22% and superior operational stability over 2000 h, *ACS Appl. Mater. Interfaces*, 2019, **11**, 39998–40005.
- 19 H. Zhou, Q. Chen, G. Li, S. Luo, T.-b. Song, H.-S. Duan, Z. Hong, J. You, Y. Liu and Y. Yang, Interface engineering of highly efficient perovskite solar cells, *Science*, 2014, **345**, 542–546.
- 20 W. Chen, Y. Wu, J. Fan, A. B. Djurišić, F. Liu, H. W. Tam, A. Ng, C. Surya, W. K. Chan and D. Wang, Understanding the doping effect on NiO: toward high-performance inverted perovskite solar cells, *Adv. Energy Mater.*, 2018, **8**, 1703519.
- 21 W. Chen, Y. Zhou, G. Chen, Y. Wu, B. Tu, F. Z. Liu, L. Huang, A. M. C. Ng, A. B. Djurišić and Z. He, Alkali chlorides for the suppression of the interfacial recombination in inverted planar perovskite solar cells, *Adv. Energy Mater.*, 2019, **9**, 1803872.



- 22 J. Song, L. Zhao, S. Huang, X. Yan, Q. Qiu, Y. Zhao, L. Zhu, Y. Qiang, H. Li and G. Li, A p-p+ Homo Junction-Enhanced Hole Transfer in Inverted Planar Perovskite Solar Cells, *ChemSusChem*, 2021, **14**, 1396–1403.
- 23 H. Min, D. Y. Lee, J. Kim, G. Kim, K. S. Lee, J. Kim and S. Il Seok, Perovskite solar cells with atomically coherent interlayers on SnO₂ electrodes, *Nature*, 2021, **598**(7881), 444–450.
- 24 P. K. Kung, M. H. Li, P. Y. Lin, Y. H. Chiang, C. R. Chan, T. F. Guo and P. Chen, A review of inorganic hole transport materials for perovskite solar cells, *Adv. Mater. Interfaces*, 2018, **5**, 1800882.
- 25 K. K. Bass, R. E. McAnally, S. Zhou, P. I. Djurovich, M. E. Thompson and B. C. Melot, Influence of moisture on the preparation, crystal structure, and photophysical properties of organohalide perovskites, *Chem. Commun.*, 2014, **50**, 15819–15822.
- 26 E. Edri, S. Kirmayer, A. Henning, S. Mukhopadhyay, K. Gartsman, Y. Rosenwaks, G. Hodes and D. Cahen, Why lead methylammonium tri-iodide perovskite-based solar cells require a mesoporous electron transporting scaffold (but not necessarily a hole conductor), *Nano Lett.*, 2014, **14**, 1000–1004.
- 27 D. Bryant, N. Aristidou, S. Pont, I. Sanchez-Molina, T. Chotchunangatchaval, S. Wheeler, J. R. Durrant and S. A. Haque, Light and oxygen induced degradation limits the operational stability of methylammonium lead triiodide perovskite solar cells, *Energy Environ. Sci.*, 2016, **9**, 1655–1660.
- 28 M. Saliba, T. Matsui, J.-Y. Seo, K. Domanski, J.-P. Correa-Baena, M. K. Nazeeruddin, S. M. Zakeeruddin, W. Tress, A. Abate and A. Hagfeldt, Cesium-containing triple cation perovskite solar cells: improved stability, reproducibility and high efficiency, *Energy Environ. Sci.*, 2016, **9**, 1989–1997.
- 29 W. Li, W. Zhang, S. Van Reenen, R. J. Sutton, J. Fan, A. A. Haghighirad, M. B. Johnston, L. Wang and H. J. Snaith, Enhanced UV-light stability of planar heterojunction perovskite solar cells with caesium bromide interface modification, *Energy Environ. Sci.*, 2016, **9**, 490–498.
- 30 F. T. O'Mahony, Y. H. Lee, C. Jellett, S. Dmitrov, D. T. Bryant, J. R. Durrant, B. C. O'Regan, M. Graetzel, M. K. Nazeeruddin and S. A. Haque, Improved environmental stability of organic lead trihalide perovskite-based photoactive-layers in the presence of mesoporous TiO₂, *J. Mater. Chem. A*, 2015, **3**, 7219–7223.
- 31 N. Chander, A. Khan, P. Chandrasekhar, E. Thouti, S. K. Swami, V. Dutta and V. K. Komarala, Reduced ultraviolet light induced degradation and enhanced light harvesting using YVO₄: Eu³⁺ down-shifting nanophosphor layer in organometal halide perovskite solar cells, *Appl. Phys. Lett.*, 2014, **105**, 033904.
- 32 X. Zhao and N.-G. Park, Stability issues on perovskite solar cells, in *Proceedings of the Photonics*, 2015, pp. 1139–1151.
- 33 J. Wang, Y. Chen, M. Liang, G. Ge, R. Zhou, Z. Sun and S. Xue, A new thermal-stable truxene-based hole-transporting material for perovskite solar cells, *Dyes Pigm.*, 2016, **125**, 399–406.
- 34 B. Philippe, B.-W. Park, R. Lindblad, J. Oscarsson, S. Ahmadi, E. M. Johansson and H. Rensmo, Chemical and Electronic Structure Characterization of Lead Halide Perovskites and Stability Behavior under Different Exposures A Photoelectron Spectroscopy Investigation, *Chem. Mater.*, 2015, **27**, 1720–1731.
- 35 A. Djurišić, F. Liu, A. M. Ng, Q. Dong, M. K. Wong, A. Ng and C. Surya, Stability issues of the next generation solar cells, *Phys. Status Solidi RRL*, 2016, **10**, 281–299.
- 36 M. Zhang, H. Yu, M. Lyu, Q. Wang, J.-H. Yun and L. Wang, Composition-dependent photoluminescence intensity and prolonged recombination lifetime of perovskite CH₃ NH₃ PbBr_{3-x} Cl_x films, *Chem. Commun.*, 2014, **50**, 11727–11730.
- 37 L. Badia, E. Mas-Marzá, R. S. Sánchez, E. M. Barea, J. Bisquert and I. Mora-Seró, New iridium complex as additive to the spiro-OMeTAD in perovskite solar cells with enhanced stability, *APL Mater.*, 2014, **2**, 081507.
- 38 Y. S. Kwon, J. Lim, H.-J. Yun, Y.-H. Kim and T. Park, A diketopyrrolopyrrole-containing hole transporting conjugated polymer for use in efficient stable organic-inorganic hybrid solar cells based on a perovskite, *Energy Environ. Sci.*, 2014, **7**, 1454–1460.
- 39 E. L. Unger, E. T. Hoke, C. D. Bailie, W. H. Nguyen, A. R. Bowring, T. Heumüller, M. G. Christoforo and M. D. McGehee, Hysteresis and transient behavior in current-voltage measurements of hybrid-perovskite absorber solar cells, *Energy Environ. Sci.*, 2014, **7**, 3690–3698.
- 40 I. Hwang, I. Jeong, J. Lee, M. J. Ko and K. Yong, Enhancing stability of perovskite solar cells to moisture by the facile hydrophobic passivation, *ACS Appl. Mater. Interfaces*, 2015, **7**, 17330–17336.
- 41 W. H. Nguyen, C. D. Bailie, E. L. Unger and M. D. McGehee, Enhancing the hole-conductivity of spiro-OMeTAD without oxygen or lithium salts by using spiro (TFPI) 2 in perovskite and dye-sensitized solar cells, *J. Am. Chem. Soc.*, 2014, **136**, 10996–11001.
- 42 D. Wang, M. Wright, N. K. Elumalai and A. Uddin, Stability of perovskite solar cells, *Sol. Energy Mater. Sol. Cells*, 2016, **147**, 255–275.
- 43 F. Machui, M. Hösel, N. Li, G. D. Spyropoulos, T. Ameri, R. R. Søndergaard, M. Jørgensen, A. Scheel, D. Gaiser and K. Kreul, Cost analysis of roll-to-roll fabricated ITO free single and tandem organic solar modules based on data from manufacture, *Energy Environ. Sci.*, 2014, **7**, 2792–2802.
- 44 A. Rivaton, S. Chambon, M. Manceau, J.-L. Gardette, N. Lemaître and S. Guillerez, Light-induced degradation of the active layer of polymer-based solar cells, *Polym. Degrad. Stab.*, 2010, **95**, 278–284.
- 45 T. M. Koh, K. Fu, Y. Fang, S. Chen, T. C. Sum, N. Mathews, S. G. Mhaisalkar, P. P. Boix and T. Baikie, Formamidinium-containing metal-halide: an alternative material for near-IR absorption perovskite solar cells, *J. Phys. Chem. C*, 2014, **118**, 16458–16462.



- 46 J. Yin, J. Cao, X. He, S. Yuan, S. Sun, J. Li, N. Zheng and L. Lin, Improved stability of perovskite solar cells in ambient air by controlling the mesoporous layer, *J. Mater. Chem. A*, 2015, **3**, 16860–16866.
- 47 I. C. Smith, E. T. Hoke, D. Solis-Ibarra, M. D. McGehee and H. I. Karunadasa, A layered hybrid perovskite solar-cell absorber with enhanced moisture stability, *Angew. Chem., Int. Ed.*, 2014, **53**, 11232–11235.
- 48 K. Mahmood, S. Sarwar and M. T. Mehran, Current status of electron transport layers in perovskite solar cells: materials and properties, *RSC Adv.*, 2017, **7**, 17044–17062.
- 49 T. Kim, J. Lim and S. Song, Recent progress and challenges of electron transport layers in organic–inorganic perovskite solar cells, *Energies*, 2020, **13**, 5572.
- 50 S. Nair and J. V. Gohel, A Review on Contemporary Hole Transport Materials for Perovskite Solar Cells, *Nanotechnology for Energy and Environmental Engineering*, 2020, pp. 145–168.
- 51 K. Hwang, Y. S. Jung, Y. J. Heo, F. H. Scholes, S. E. Watkins, J. Subbiah, D. J. Jones, D. Y. Kim and D. Vak, Toward large scale roll-to-roll production of fully printed perovskite solar cells, *Adv. Mater.*, 2015, **27**, 1241–1247.
- 52 T. M. Schmidt, T. T. Larsen-Olsen, J. E. Carlé, D. Angmo and F. C. Krebs, Upscaling of perovskite solar cells: fully ambient roll processing of flexible perovskite solar cells with printed back electrodes, *Adv. Energy Mater.*, 2015, **5**, 1500569.
- 53 C. Grätzel and S. M. Zakeeruddin, Recent trends in mesoscopic solar cells based on molecular and nanopigment light harvesters, *Mater. Today*, 2013, **16**, 11–18.
- 54 H.-S. Kim, C.-R. Lee, J.-H. Im, K.-B. Lee, T. Moehl, A. Marchioro, S.-J. Moon, R. Humphry-Baker, J.-H. Yum and J. E. Moser, Lead iodide perovskite sensitized all-solid-state submicron thin film mesoscopic solar cell with efficiency exceeding 9%, *Sci. Rep.*, 2012, **2**, 1–7.
- 55 Z. Liu, M. Zhang, X. Xu, L. Bu, W. Zhang, W. Li, Z. Zhao, M. Wang, Y.-B. Cheng and H. He, p-Type mesoscopic NiO as an active interfacial layer for carbon counter electrode based perovskite solar cells, *Dalton Trans.*, 2015, **44**, 3967–3973.
- 56 F. Di Giacomo, V. Zardetto, A. D'Epifanio, S. Pescetelli, F. Matteocci, S. Razza, A. Di Carlo, S. Licoccia, W. M. Kessels and M. Creatore, Flexible perovskite photovoltaic modules and solar cells based on atomic layer deposited compact layers and UV-irradiated TiO₂ scaffolds on plastic substrates, *Adv. Energy Mater.*, 2015, **5**, 1401808.
- 57 A. Kojima, K. Teshima, Y. Shirai and T. Miyasaka, Organometal halide perovskites as visible-light sensitizers for photovoltaic cells, *J. Am. Chem. Soc.*, 2009, **131**, 6050–6051.
- 58 S. Dharani, H. K. Mulmudi, N. Yantara, P. T. T. Trang, N. G. Park, M. Graetzel, S. Mhaisalkar, N. Mathews and P. P. Boix, High efficiency electrospun TiO₂ nanofiber based hybrid organic–inorganic perovskite solar cell, *Nanoscale*, 2014, **6**, 1675–1679.
- 59 J. H. Noh, S. H. Im, J. H. Heo, T. N. Mandal and S. I. Seok, Chemical management for colorful, efficient, and stable inorganic–organic hybrid nanostructured solar cells, *Nano Lett.*, 2013, **13**, 1764–1769.
- 60 T. Leijtens, B. Lauber, G. E. Eperon, S. D. Stranks and H. J. Snaith, The importance of perovskite pore filling in organometal mixed halide sensitized TiO₂-based solar cells, *J. Phys. Chem. Lett.*, 2014, **5**, 1096–1102.
- 61 K. Mahmood, B. S. Swain and H. S. Jung, Controlling the surface nanostructure of ZnO and Al-doped ZnO thin films using electrostatic spraying for their application in 12% efficient perovskite solar cells, *Nanoscale*, 2014, **6**, 9127–9138.
- 62 J. M. Ball, M. M. Lee, A. Hey and H. J. Snaith, Low-temperature processed meso-superstructured to thin-film perovskite solar cells, *Energy Environ. Sci.*, 2013, **6**, 1739–1743.
- 63 J. Y. Kim, The Stability Effect of Atomic Layer Deposition (ALD) of Al₂O₃ on CH₃NH₃PbI₃ Perovskite Solar Cell Fabricated by Vapor Deposition, in *Proceedings of the Key Engineering Materials*, 2017, pp. 156–162.
- 64 B. J. Kim, S. Lee and H. S. Jung, Recent progressive efforts in perovskite solar cells toward commercialization, *J. Mater. Chem. A*, 2018, **6**, 12215–12236.
- 65 T. Matsui, J. Y. Seo, M. Saliba, S. M. Zakeeruddin and M. Grätzel, Room-Temperature Formation of Highly Crystalline Multication Perovskites for Efficient, Low-Cost Solar Cells, *Adv. Mater.*, 2017, **29**, 1606258.
- 66 L. Yang, A. T. Barrows, D. G. Lidzey and T. Wang, Recent progress and challenges of organometal halide perovskite solar cells, *Rep. Prog. Phys.*, 2016, **79**, 026501.
- 67 Q. Qin, Z. Zhang, Y. Cai, Y. Zhou, H. Liu, X. Lu, X. Gao, L. Shui, S. Wu and J. Liu, Improving the performance of low-temperature planar perovskite solar cells by adding functional fullerene end-capped polyethylene glycol derivatives, *J. Power Sources*, 2018, **396**, 49–56.
- 68 H. Dong, Z. Wu, J. Xi, X. Xu, L. Zuo, T. Lei, X. Zhao, L. Zhang, X. Hou and A. K. Y. Jen, Pseudohalide-induced recrystallization engineering for CH₃NH₃PbI₃ film and its application in highly efficient inverted planar heterojunction perovskite solar cells, *Adv. Funct. Mater.*, 2018, **28**, 1704836.
- 69 Z. Yu and L. Sun, Recent progress on hole-transporting materials for emerging organometal halide perovskite solar cells, *Adv. Energy Mater.*, 2015, **5**, 1500213.
- 70 F. Xie, C.-C. Chen, Y. Wu, X. Li, M. Cai, X. Liu, X. Yang and L. Han, Vertical recrystallization for highly efficient and stable formamidinium-based inverted-structure perovskite solar cells, *Energy Environ. Sci.*, 2017, **10**, 1942–1949.
- 71 E. H. Anaraki, A. Kermanpur, L. Steier, K. Domanski, T. Matsui, W. Tress, M. Saliba, A. Abate, M. Grätzel and A. Hagfeldt, Highly efficient and stable planar perovskite solar cells by solution-processed tin oxide, *Energy Environ. Sci.*, 2016, **9**, 3128–3134.
- 72 D. Luo, W. Yang, Z. Wang, A. Sadhanala, Q. Hu, R. Su, R. Shivanna, G. F. Trindade, J. F. Watts and Z. Xu,



- Enhanced photovoltage for inverted planar heterojunction perovskite solar cells, *Science*, 2018, **360**, 1442–1446.
- 73 J. Y. Seo, T. Matsui, J. Luo, J. P. Correa-Baena, F. Giordano, M. Saliba, K. Schenk, A. Ummadisingu, K. Domanski and M. Hadadian, Ionic liquid control crystal growth to enhance planar perovskite solar cells efficiency, *Adv. Energy Mater.*, 2016, **6**, 1600767.
 - 74 X. Crispin, F. Jakobsson, A. Crispin, P. Grim, P. Andersson, A. v. Volodin, C. Van Haesendonck, M. Van der Auweraer, W. R. Salaneck and M. Berggren, The origin of the high conductivity of poly (3,4-ethylenedioxythiophene)-poly (styrenesulfonate)(PEDOT-PSS) plastic electrodes, *Chem. Mater.*, 2006, **18**, 4354–4360.
 - 75 S. Sun, T. Salim, N. Mathews, M. Duchamp, C. Boothroyd, G. Xing, T. C. Sum and Y. M. Lam, The origin of high efficiency in low-temperature solution-processable bilayer organometal halide hybrid solar cells, *Energy Environ. Sci.*, 2014, **7**, 399–407.
 - 76 J. Y. Jeng, Y. F. Chiang, M. H. Lee, S. R. Peng, T. F. Guo, P. Chen and T. C. Wen, CH₃NH₃PbI₃ perovskite/fullerene planar-heterojunction hybrid solar cells, *Adv. Mater.*, 2013, **25**, 3727–3732.
 - 77 Y. Liu, Q. Chen, H.-S. Duan, H. Zhou, Y. M. Yang, H. Chen, S. Luo, T.-B. Song, L. Dou and Z. Hong, A dopant-free organic hole transport material for efficient planar heterojunction perovskite solar cells, *J. Mater. Chem. A*, 2015, **3**, 11940–11947.
 - 78 J. H. Heo, H. J. Han, D. Kim, T. K. Ahn and S. H. Im, Hysteresis-less inverted CH₃NH₃PbI₃ planar perovskite hybrid solar cells with 18.1% power conversion efficiency, *Energy Environ. Sci.*, 2015, **8**, 1602–1608.
 - 79 S. Shi, Y. Li, X. Li and H. Wang, Advancements in all-solid-state hybrid solar cells based on organometal halide perovskites, *Mater. Horiz.*, 2015, **2**, 378–405.
 - 80 Q. Wang, C.-C. Chueh, M. Eslamian and A. K.-Y. Jen, Modulation of PEDOT: PSS pH for efficient inverted perovskite solar cells with reduced potential loss and enhanced stability, *ACS Appl. Mater. Interfaces*, 2016, **8**, 32068–32076.
 - 81 J. Huang, K.-X. Wang, J.-J. Chang, Y.-Y. Jiang, Q.-S. Xiao and Y. Li, Improving the efficiency and stability of inverted perovskite solar cells with dopamine-copolymerized PEDOT: PSS as a hole extraction layer, *J. Mater. Chem. A*, 2017, **5**, 13817–13822.
 - 82 L. Hu, K. Sun, M. Wang, W. Chen, B. Yang, J. Fu, Z. Xiong, X. Li, X. Tang and Z. Zang, Inverted planar perovskite solar cells with a high fill factor and negligible hysteresis by the dual effect of NaCl-doped PEDOT: PSS, *ACS Appl. Mater. Interfaces*, 2017, **9**, 43902–43909.
 - 83 C.-H. Chiang, Z.-L. Tseng and C.-G. Wu, Planar heterojunction perovskite/PC 71 BM solar cells with enhanced open-circuit voltage via a (2/1)-step spin-coating process, *J. Mater. Chem. A*, 2014, **2**, 15897–15903.
 - 84 S. Pang, D. Chen, C. Zhang, J. Chang, Z. Lin, H. Yang, X. Sun, J. Mo, H. Xi and G. Han, Efficient bifacial semitransparent perovskite solar cells with silver thin film electrode, *Sol. Energy Mater. Sol. Cells*, 2017, **170**, 278–286.
 - 85 Q. Jiang, Y. Zhao, X. Zhang, X. Yang, Y. Chen, Z. Chu, Q. Ye, X. Li, Z. Yin and J. You, Surface passivation of perovskite film for efficient solar cells, *Nat. Photonics*, 2019, **13**, 460–466.
 - 86 N. Arora, M. I. Dar, A. Hinderhofer, N. Pellet, F. Schreiber, S. M. Zakeeruddin and M. Grätzel, Perovskite solar cells with CuSCN hole extraction layers yield stabilized efficiencies greater than 20%, *Science*, 2017, **358**, 768–771.
 - 87 J. W. Jung, C. C. Chueh and A. K. Y. Jen, A low-temperature, solution-processable, Cu-doped nickel oxide hole-transporting layer via the combustion method for high-performance thin-film perovskite solar cells, *Adv. Mater.*, 2015, **27**, 7874–7880.
 - 88 W. Sun, Y. Li, S. Ye, H. Rao, W. Yan, H. Peng, Y. Li, Z. Liu, S. Wang and Z. Chen, High-performance inverted planar heterojunction perovskite solar cells based on a solution-processed CuO x hole transport layer, *Nanoscale*, 2016, **8**, 10806–10813.
 - 89 M. Huangfu, Y. Shen, G. Zhu, K. Xu, M. Cao, F. Gu and L. Wang, Copper iodide as inorganic hole conductor for perovskite solar cells with different thickness of mesoporous layer and hole transport layer, *Appl. Surf. Sci.*, 2015, **357**, 2234–2240.
 - 90 H. Zhang, H. Wang, W. Chen and A. K. Y. Jen, CuGaO₂: A promising inorganic hole-transporting material for highly efficient and stable perovskite solar cells, *Adv. Mater.*, 2017, **29**, 1604984.
 - 91 F. Igbari, M. Li, Y. Hu, Z.-K. Wang and L.-S. Liao, A room-temperature CuAlO₂ hole interfacial layer for efficient and stable planar perovskite solar cells, *J. Mater. Chem. A*, 2016, **4**, 1326–1335.
 - 92 H. Sung, N. Ahn, M. S. Jang, J. K. Lee, H. Yoon, N. G. Park and M. Choi, Transparent conductive oxide-free graphene-based perovskite solar cells with over 17% efficiency, *Adv. Energy Mater.*, 2016, **6**, 1501873.
 - 93 H. Rao, W. Sun, S. Ye, W. Yan, Y. Li, H. Peng, Z. Liu, Z. Bian and C. Huang, Solution-processed CuS NPs as an inorganic hole-selective contact material for inverted planar perovskite solar cells, *ACS Appl. Mater. Interfaces*, 2016, **8**, 7800–7805.
 - 94 E. Singh, K. S. Kim, G. Y. Yeom and H. S. Nalwa, Atomically thin-layered molybdenum disulfide (MoS₂) for bulk-heterojunction solar cells, *ACS Appl. Mater. Interfaces*, 2017, **9**, 3223–3245.
 - 95 D. Yao, *Interfacial and compositional engineering of perovskite solar cells for enhanced device performance and stability*, Queensland University of Technology, 2020.
 - 96 A. Al Mamun, T. T. Ava, K. Zhang, H. Baumgart and G. Namkoong, New PCBM/carbon based electron transport layer for perovskite solar cells, *Phys. Chem. Chem. Phys.*, 2017, **19**, 17960–17966.
 - 97 K. Aitola, K. Sveinbjörnsson, J.-P. Correa-Baena, A. Kaskela, A. Abate, Y. Tian, E. M. Johansson, M. Grätzel, E. I. Kauppinen and A. Hagfeldt, Carbon nanotube-based hybrid hole-transporting material and selective contact for high efficiency perovskite solar cells, *Energy Environ. Sci.*, 2016, **9**, 461–466.



- 98 J. Cao, Y.-M. Liu, X. Jing, J. Yin, J. Li, B. Xu, Y.-Z. Tan and N. Zheng, Well-defined thiolated nanographene as hole-transporting material for efficient and stable perovskite solar cells, *J. Am. Chem. Soc.*, 2015, **137**, 10914–10917.
- 99 R. Singh, H. Jun and A. K. Arof, Activated carbon as back contact for HTM-free mixed cation perovskite solar cell, *Phase Transitions*, 2018, **91**, 1268–1276.
- 100 W. S. Yang, B.-W. Park, E. H. Jung, N. J. Jeon, Y. C. Kim, D. U. Lee, S. S. Shin, J. Seo, E. K. Kim and J. H. Noh, Iodide management in formamidinium-lead-halide-based perovskite layers for efficient solar cells, *Science*, 2017, **356**, 1376–1379.
- 101 T. H. Chowdhury, M. Akhtaruzzaman, M. E. Kayesh, R. Kaneko, T. Noda, J.-J. Lee and A. Islam, Low temperature processed inverted planar perovskite solar cells by r-GO/CuSCN hole-transport bilayer with improved stability, *Sol. Energy*, 2018, **171**, 652–657.
- 102 J.-S. Yeo, C.-H. Lee, D. Jang, S. Lee, S. M. Jo, H.-I. Joh and D.-Y. Kim, Reduced graphene oxide-assisted crystallization of perovskite *via* solution-process for efficient and stable planar solar cells with module-scales, *Nano Energy*, 2016, **30**, 667–676.
- 103 Z. Zhou, X. Li, M. Cai, F. Xie, Y. Wu, Z. Lan, X. Yang, Y. Qiang, A. Islam and L. Han, Stable inverted planar perovskite solar cells with low-temperature-processed hole-transport bilayer, *Adv. Energy Mater.*, 2017, **7**, 1700763.
- 104 M. Que, B. Zhang, J. Chen, X. Yin and S. Yun, Carbon-based electrodes for perovskite solar cells, *Mater. Adv.*, 2021, **2**, 5560–5579.
- 105 L. Q. Zhang, X. W. Zhang, Z. G. Yin, Q. Jiang, X. Liu, J. H. Meng, Y. J. Zhao and H. L. Wang, Highly efficient and stable planar heterojunction perovskite solar cells *via* a low temperature solution process, *J. Mater. Chem. A*, 2015, **3**, 12133–12138.
- 106 S. Ravishankar, S. Gharibzadeh, C. Roldán-Carmona, G. Grancini, Y. Lee, M. Ralaifarisoa, A. M. Asiri, N. Koch, J. Bisquert and M. K. Nazeeruddin, Influence of charge transport layers on open-circuit voltage and hysteresis in perovskite solar cells, *Joule*, 2018, **2**, 788–798.
- 107 W.-Q. Wu, Q. Wang, Y. Fang, Y. Shao, S. Tang, Y. Deng, H. Lu, Y. Liu, T. Li and Z. Yang, Molecular doping enabled scalable blading of efficient hole-transport-layer-free perovskite solar cells, *Nat. Commun.*, 2018, **9**, 1–8.
- 108 Q. Jiang, X. Zhang and J. You, SnO₂: a wonderful electron transport layer for perovskite solar cells, *Small*, 2018, **14**, 1801154.
- 109 S. S. Shin, E. J. Yeom, W. S. Yang, S. Hur, M. G. Kim, J. Im, J. Seo, J. H. Noh and S. I. Seok, Colloidally prepared La-doped BaSnO₃ electrodes for efficient, photostable perovskite solar cells, *Science*, 2017, **356**, 167–171.
- 110 M. M. Lee, J. Teuscher, T. Miyasaka, T. N. Murakami and H. J. Snaith, Efficient hybrid solar cells based on meso-superstructured organometal halide perovskites, *Science*, 2012, **338**, 643–647.
- 111 G. Xing, N. Mathews, S. Sun, S. S. Lim, Y. M. Lam, M. Grätzel, S. Mhaisalkar and T. C. Sum, Long-range balanced electron-and hole-transport lengths in organic-inorganic CH₃NH₃PbI₃, *Science*, 2013, **342**, 344–347.
- 112 Z. Zhou and S. Pang, Highly efficient inverted hole-transport-layer-free perovskite solar cells, *J. Mater. Chem. A*, 2020, **8**, 503–512.
- 113 S. D. Stranks, G. E. Eperon, G. Grancini, C. Menelaou, M. J. Alcocer, T. Leijtens, L. M. Herz, A. Petrozza and H. J. Snaith, Electron-hole diffusion lengths exceeding 1 micrometer in an organometal trihalide perovskite absorber, *Science*, 2013, **342**, 341–344.
- 114 C. Sun, Z. Wu, H. L. Yip, H. Zhang, X. F. Jiang, Q. Xue, Z. Hu, Z. Hu, Y. Shen and M. Wang, Amino-functionalized conjugated polymer as an efficient electron transport layer for high-performance planar-heterojunction perovskite solar cells, *Adv. Energy Mater.*, 2016, **6**, 1501534.
- 115 X. Zhou, L. Zhang, H. Hu, Z. Jiang, D. Wang, J. Chen and B. Xu, Highly Efficient and Stable Hole-Transport-Layer-Free Inverted Perovskite Solar Cells Achieved 22% Efficiency Through P-type Molecular Synergistic Doping, *Nano Energy*, 2022, **104**, 107988.
- 116 W. Chen, X. Yin, M. Que, H. Xie, J. Liu, C. Yang, Y. Guo, Y. Wu and W. Que, A comparative study of planar and mesoporous perovskite solar cells with printable carbon electrodes, *J. Power Sources*, 2019, **412**, 118–124.
- 117 L. Etgar, P. Gao, Z. Xue, Q. Peng, A. K. Chandiran, B. Liu, M. K. Nazeeruddin and M. Grätzel, Mesoscopic CH₃NH₃PbI₃/TiO₂ heterojunction solar cells, *J. Am. Chem. Soc.*, 2012, **134**, 17396–17399.
- 118 W. A. Laban and L. Etgar, Depleted hole conductor-free lead halide iodide heterojunction solar cells, *Energy Environ. Sci.*, 2013, **6**, 3249–3253.
- 119 S. Aharon, S. Gamliel, B. El Cohen and L. Etgar, Depletion region effect of highly efficient hole conductor free CH₃NH₃PbI₃ perovskite solar cells, *Phys. Chem. Chem. Phys.*, 2014, **16**, 10512–10518.
- 120 H. Wei, J. Xiao, Y. Yang, S. Lv, J. Shi, X. Xu, J. Dong, Y. Luo, D. Li and Q. Meng, Free-standing flexible carbon electrode for highly efficient hole-conductor-free perovskite solar cells, *Carbon*, 2015, **93**, 861–868.
- 121 Q. Ma, S. Huang, X. Wen, M. A. Green and A. W. Ho-Baillie, Hole transport layer free inorganic CsPbI₂Br₂ perovskite solar cell by dual source thermal evaporation, *Adv. Energy Mater.*, 2016, **6**, 1502202.
- 122 F. Wan, X. Qiu, H. Chen, Y. Liu, H. Xie, J. Shi, H. Huang, Y. Yuan, Y. Gao and C. Zhou, Accelerated electron extraction and improved UV stability of TiO₂ based perovskite solar cells by SnO₂ based surface passivation, *Org. Electron.*, 2018, **59**, 184–189.
- 123 Y. Xiao, C. Wang, K. K. Kondamareddy, N. Cheng, P. Liu, Y. Qiu, F. Qi, S. Kong, W. Liu and X.-Z. Zhao, Efficient electron transport scaffold made up of submicron TiO₂ spheres for high-performance hole-transport material free perovskite solar cells, *ACS Appl. Energy Mater.*, 2018, **1**, 5453–5462.
- 124 Y. Wang, H. Zhao, Y. Mei, H. Liu, S. Wang and X. Li, Carbon nanotube bridging method for hole transport layer-free



- paintable carbon-based perovskite solar cells, *ACS Appl. Mater. Interfaces*, 2018, **11**, 916–923.
- 125 F. Li, C. Wang, P. Liu, Y. Xiao, L. Bai, F. Qi, X. Hou, H. Zhang, Y. Wang and S. Wang, Fully air-processed carbon-based efficient hole conductor free planar heterojunction perovskite solar cells with high reproducibility and stability, *Sol. RRL*, 2019, **3**, 1800297.
 - 126 Y. Yang, Z. Liu, W. K. Ng, L. Zhang, H. Zhang, X. Meng, Y. Bai, S. Xiao, T. Zhang and C. Hu, An ultrathin ferroelectric perovskite oxide layer for high-performance hole transport material free carbon based halide perovskite solar cells, *Adv. Funct. Mater.*, 2019, **29**, 1806506.
 - 127 K.-W. Tsai, C.-C. Chueh, S. T. Williams, T.-C. Wen and A. K. Jen, High-performance hole-transporting layer-free conventional perovskite/fullerene heterojunction thin-film solar cells, *J. Mater. Chem. A*, 2015, **3**, 9128–9132.
 - 128 Y. Li, S. Ye, W. Sun, W. Yan, Y. Li, Z. Bian, Z. Liu, S. Wang and C. Huang, Hole-conductor-free planar perovskite solar cells with 16.0% efficiency, *J. Mater. Chem. A*, 2015, **3**, 18389–18394.
 - 129 S. Ye, H. Rao, W. Yan, Y. Li, W. Sun, H. Peng, Z. Liu, Z. Bian, Y. Li and C. Huang, A strategy to simplify the preparation process of perovskite solar cells by co-deposition of a hole-conductor and a perovskite layer, *Adv. Mater.*, 2016, **28**, 9648–9654.
 - 130 S. Ye, H. Rao, Z. Zhao, L. Zhang, H. Bao, W. Sun, Y. Li, F. Gu, J. Wang and Z. Liu, A breakthrough efficiency of 19.9% obtained in inverted perovskite solar cells by using an efficient trap state passivator Cu (thiourea) I, *J. Am. Chem. Soc.*, 2017, **139**, 7504–7512.
 - 131 Z. Zhou, Z. Qiang, T. Sakamaki, I. Takei, R. Shang and E. Nakamura, Organic/Inorganic Hybrid p-Type Semiconductor Doping Affords Hole Transporting Layer Free Thin-Film Perovskite Solar Cells with High Stability, *ACS Appl. Mater. Interfaces*, 2019, **11**, 22603–22611.
 - 132 K. Schutt, P. K. Nayak, A. J. Ramadan, B. Wenger, Y. H. Lin and H. J. Snaith, Overcoming zinc oxide interface instability with a methylammonium-free perovskite for high-performance solar cells, *Adv. Funct. Mater.*, 2019, **29**, 1900466.
 - 133 S. A. Weber, I. M. Hermes, S.-H. Turren-Cruz, C. Gort, V. W. Bergmann, L. Gilson, A. Hagfeldt, M. Graetzel, W. Tress and R. Berger, How the formation of interfacial charge causes hysteresis in perovskite solar cells, *Energy Environ. Sci.*, 2018, **11**, 2404–2413.
 - 134 A. Uddin and H. Yi, Progress and challenges of SnO₂ electron transport layer for perovskite solar cells: A critical review, *Sol. RRL*, 2022, 2100983.
 - 135 L. Huang, J. Xu, X. Sun, Y. Du, H. Cai, J. Ni, J. Li, Z. Hu and J. Zhang, Toward revealing the critical role of perovskite coverage in highly efficient electron-transport layer-free perovskite solar cells: an energy band and equivalent circuit model perspective, *ACS Appl. Mater. Interfaces*, 2016, **8**, 9811–9820.
 - 136 Q. Han, J. Ding, Y. Bai, T. Li, J.-Y. Ma, Y.-X. Chen, Y. Zhou, J. Liu, Q.-Q. Ge and J. Chen, Carrier dynamics engineering for high-performance electron-transport-layer-free perovskite photovoltaics, *Chem*, 2018, **4**, 2405–2417.
 - 137 D. Liu, J. Yang and T. L. Kelly, Compact layer free perovskite solar cells with 13.5% efficiency, *J. Am. Chem. Soc.*, 2014, **136**, 17116–17122.
 - 138 W. Ke, G. Fang, J. Wan, H. Tao, Q. Liu, L. Xiong, P. Qin, J. Wang, H. Lei and G. Yang, Efficient hole-blocking layer-free planar halide perovskite thin-film solar cells, *Nat. Commun.*, 2015, **6**, 1–7.
 - 139 W. Chen, X. Bao, Q. Zhu, D. Zhu, M. Qiu, M. Sun and R. Yang, Simple planar perovskite solar cells with a dopant-free benzodithiophene conjugated polymer as hole transporting material, *J. Mater. Chem. C*, 2015, **3**, 10070–10073.
 - 140 J. Pascual, I. Kosta, T. Tuyen Ngo, A. Chuvilin, G. Cabanero, H. J. Grande, E. M. Barea, I. Mora-Seró, J. L. Delgado and R. Tena-Zaera, Electron Transport Layer-Free Solar Cells Based on Perovskite–Fullerene Blend Films with Enhanced Performance and Stability, *ChemSusChem*, 2016, **9**, 2679–2685.
 - 141 T. Shi, J. Chen, J. Zheng, X. Li, B. Zhou, H. Cao and Y. Wang, Ti/Au Cathode for Electronic transport material-free organic-inorganic hybrid perovskite solar cells, *Sci. Rep.*, 2016, **6**, 1–6.
 - 142 P. Cui, D. Wei, J. Ji, D. Song, Y. Li, X. Liu, J. Huang, T. Wang, J. You and M. Li, Highly efficient electron-selective layer free perovskite solar cells by constructing effective p–n heterojunction, *Sol. RRL*, 2017, **1**, 1600027.
 - 143 R. Sandoval-Torrientes, J. Pascual, I. García-Benito, S. Collavini, I. Kosta, R. Tena-Zaera, N. Martín and J. L. Delgado, Modified Fullerenes for Efficient Electron Transport Layer-Free Perovskite/Fullerene Blend-Based Solar Cells, *ChemSusChem*, 2017, **10**, 2023–2029.
 - 144 F. Huang, Y. Wei, L. Gu, Q. Guo, H. Xu, D. Luo, S. Jin, X. Yang, Y. Huang and J. Wu, Interface Engineering of electron Transport Layer-Free Planar Perovskite Solar Cells with Efficiency Exceeding 15%, *Energy Technol.*, 2017, **5**, 1844–1851.
 - 145 J. Pascual, I. Kosta, E. Palacios-Lidon, A. Chuvilin, G. Grancini, M. K. Nazeeruddin, H. J. Grande, J. L. Delgado and R. n. Tena-Zaera, Co-solvent effect in the processing of the perovskite: fullerene blend films for electron transport layer-free solar cells, *J. Phys. Chem. C*, 2018, **122**, 2512–2520.
 - 146 P. Zhao, M. Han, W. Yin, X. Zhao, S. G. Kim, Y. Yan, M. Kim, Y. J. Song, N. G. Park and H. S. Jung, Insulated interlayer for efficient and photostable electron-transport-layer-free perovskite solar cells, *ACS Appl. Mater. Interfaces*, 2018, **10**, 10132–10140.
 - 147 X. Wei, M. Zhang, X. Liu, F. Chen, X. Lei, H. Liu, F. Meng, H. Zeng, S. Yang and J. Liu, Semitransparent CH₃NH₃PbI₃ Films Achieved by Solvent Engineering for Annealing-and Electron Transport Layer-Free Planar Perovskite Solar Cells, *Sol. RRL*, 2018, **2**, 1700222.
 - 148 L. Huang, S. Bu, D. Zhang, R. Peng, Q. Wei, Z. Ge and J. Zhang, Schottky/p–n Cascade Heterojunction Constructed by Intentional n-Type Doping Perovskite



- Toward Efficient Electron Layer-Free Perovskite Solar Cells, *Sol. RRL*, 2019, 3, 1800274.
- 149 C. Huang, P. Lin, N. Fu, C. Liu, B. Xu, K. Sun, D. Wang, X. Zeng and S. Ke, Facile fabrication of highly efficient ETL-free perovskite solar cells with 20% efficiency by defect passivation and interface engineering, *Chem. Commun.*, 2019, 55, 2777–2780.
 - 150 J. F. Liao, W. Q. Wu, Y. Jiang, D. B. Kuang and L. Wang, Maze-Like Halide Perovskite Films for Efficient Electron Transport Layer-Free Perovskite Solar Cells, *Sol. RRL*, 2019, 3, 1800268.
 - 151 W. Q. Wu, J. F. Liao, J. X. Zhong, Y. F. Xu, L. Wang and J. Huang, Suppressing Interfacial Charge Recombination in Electron-Transport-Layer-Free Perovskite Solar Cells to Give an Efficiency Exceeding 21%, *Angew. Chem.*, 2020, 132, 21166–21173.
 - 152 C. W. Jang, D. H. Shin and S.-H. Choi, Photostable electron-transport-layer-free flexible graphene quantum dots/perovskite solar cells by employing bathocuproine interlayer, *J. Alloys Compd.*, 2021, 886, 161355.
 - 153 H. Duan, X. Li, Y. Gou, H. Wang, L. Fan, Y. Chen, J. Yang, L. Yang and F. Wang, A two-fold interfacial electric-field strategy: boosting the performance of electron transport layer-free perovskite solar cells with low-cost and versatile inorganic acid treatment, *J. Mater. Chem. C*, 2021, 9, 12920–12927.
 - 154 T. Ameri, N. Li and C. J. Brabec, Highly efficient organic tandem solar cells: a follow up review, *Energy Environ. Sci.*, 2013, 6, 2390–2413.
 - 155 A. Al-Ashouri, E. Köhnen, B. Li, A. Magomedov, H. Hempel, P. Caprioglio, J. A. Márquez, A. B. Morales Vilches, E. Kasparavicius and J. A. Smith, Monolithic perovskite/silicon tandem solar cell with > 29% efficiency by enhanced hole extraction, *Science*, 2020, 370, 1300–1309.
 - 156 L. Zheng, Y. Xuan, J. Wang, S. Bao, X. Liu and K. Zhang, Inverted perovskite/silicon V-shaped tandem solar cells with 27.6% efficiency via self-assembled monolayer-modified nickel oxide layer, *J. Mater. Chem. A*, 2022, 10, 7251–7262.
 - 157 S. Bremner, M. Levy and C. B. Honsberg, Analysis of tandem solar cell efficiencies under AM1. 5G spectrum using a rapid flux calculation method, *Prog. Photovoltaics*, 2008, 16, 225–233.
 - 158 G. W. Adhyaksa, E. Johlin and E. C. Garnett, Nanoscale back contact perovskite solar cell design for improved tandem efficiency, *Nano Lett.*, 2017, 17, 5206–5212.
 - 159 M. H. Futscher and B. Ehrler, Efficiency limit of perovskite/Si tandem solar cells, *ACS Energy Lett.*, 2016, 1, 863–868.
 - 160 M. W. Rowell and M. D. McGehee, Transparent electrode requirements for thin film solar cell modules, *Energy Environ. Sci.*, 2011, 4, 131–134.
 - 161 M. Prosa, N. Li, N. Gasparini, M. Bolognesi, M. Seri, M. Muccini and C. J. Brabec, Revealing minor electrical losses in the interconnecting layers of organic tandem solar cells, *Adv. Mater. Interfaces*, 2017, 4, 1700776.
 - 162 Y. Cui, H. Yao, B. Gao, Y. Qin, S. Zhang, B. Yang, C. He, B. Xu and J. Hou, Fine-tuned photoactive and interconnection layers for achieving over 13% efficiency in a fullerene-free tandem organic solar cell, *J. Am. Chem. Soc.*, 2017, 139, 7302–7309.
 - 163 N. Li, D. Baran, G. D. Spyropoulos, H. Zhang, S. Berny, M. Turbiez, T. Ameri, F. C. Krebs and C. J. Brabec, Environmentally printing efficient organic tandem solar cells with high fill factors: a guideline towards 20% power conversion efficiency, *Adv. Energy Mater.*, 2014, 4, 1400084.
 - 164 M. Hauck, T. Ligthart, M. Schaap, E. Boukris and D. Brouwer, Environmental benefits of reduced electricity use exceed impacts from lead use for perovskite based tandem solar cell, *Renewable Energy*, 2017, 111, 906–913.
 - 165 I. Celik, A. B. Phillips, Z. Song, Y. Yan, R. J. Ellingson, M. J. Heben and D. Apul, Environmental analysis of perovskites and other relevant solar cell technologies in a tandem configuration, *Energy Environ. Sci.*, 2017, 10, 1874–1884.
 - 166 B. J. Kim, D. H. Kim, Y.-Y. Lee, H.-W. Shin, G. S. Han, J. S. Hong, K. Mahmood, T. K. Ahn, Y.-C. Joo and K. S. Hong, Highly efficient and bending durable perovskite solar cells: toward a wearable power source, *Energy Environ. Sci.*, 2015, 8, 916–921.
 - 167 V. Zardetto, T. M. Brown, A. Reale and A. Di Carlo, Substrates for flexible electronics: A practical investigation on the electrical, film flexibility, optical, temperature, and solvent resistance properties, *J. Polym. Sci., Part B: Polym. Phys.*, 2011, 49, 638–648.
 - 168 J. Feng, X. Zhu, Z. Yang, X. Zhang, J. Niu, Z. Wang, S. Zuo, S. Priya, S. Liu and D. Yang, Record efficiency stable flexible perovskite solar cell using effective additive assistant strategy, *Adv. Mater.*, 2018, 30, 1801418.
 - 169 L. Chao, Y. Xia, B. Li, G. Xing, Y. Chen and W. Huang, Room-temperature molten salt for facile fabrication of efficient and stable perovskite solar cells in ambient air, *Chem*, 2019, 5, 995–1006.
 - 170 J. Werner, B. Niesen and C. Ballif, Perovskite/silicon tandem solar cells: marriage of convenience or true love story?—An overview, *Adv. Mater. Interfaces*, 2018, 5, 1700731.
 - 171 Y. Li, L. Meng, Y. M. Yang, G. Xu, Z. Hong, Q. Chen, J. You, G. Li, Y. Yang and Y. Li, High-efficiency robust perovskite solar cells on ultrathin flexible substrates, *Nat. Commun.*, 2016, 7, 1–10.
 - 172 P. Guggilla, K. Bhat and E. J. Bernardez, Thin films to single crystals: organometal halide perovskite materials for advanced optoelectronics, journal of photonic materials and technology, *J. Photonic Mater. Technol.*, 2016, 2, 25–31.
 - 173 W. Peng, L. Wang, B. Murali, K. T. Ho, A. Bera, N. Cho, C. F. Kang, V. M. Burlakov, J. Pan and L. Sinatra, Solution-grown monocrystalline hybrid perovskite films for hole-transporter-free solar cells, *Adv. Mater.*, 2016, 28, 3383–3390.
 - 174 H.-S. Rao, B.-X. Chen, X.-D. Wang, D.-B. Kuang and C.-Y. Su, A micron-scale laminar MAPbBr₃ single crystal for an efficient and stable perovskite solar cell, *Chem. Commun.*, 2017, 53, 5163–5166.
 - 175 M. Shahinuzzaman, S. Afroz, H. Mohafez, M. S. Jamal, M. U. Khandaker, A. Sulieman, N. Tamam and



- M. A. Islam, Roles of Inorganic Oxide Based HTMs towards Highly Efficient and Long-Term Stable PSC—A Review, *Nanomaterials*, 2022, **12**(17), 3003.
- 176 K. P. Bhandari, J. M. Collier, R. J. Ellingson and D. S. Apul, Energy payback time (EPBT) and energy return on energy invested (EROI) of solar photovoltaic systems: A systematic review and meta-analysis, *Renewable Sustainable Energy Rev.*, 2015, **47**, 133–141.
- 177 A. Bhat, B. P. Dhamaniya, P. Chhillar, T. B. Korukonda, G. Rawat and S. K. Pathak, Analysing the prospects of perovskite solar cells within the purview of recent scientific advancements, *Crystals*, 2018, **8**, 242.
- 178 A. A. Asif, R. Singh and G. F. Alapatt, Technical and economic assessment of perovskite solar cells for large scale manufacturing, *J. Renewable Sustainable Energy*, 2015, **7**, 043120.
- 179 N.-G. Park, M. Grätzel, T. Miyasaka, K. Zhu and K. Emery, Towards stable and commercially available perovskite solar cells, *Nat. Energy*, 2016, **1**, 1–8.
- 180 B. Hailegnaw, S. Kirmayer, E. Edri, G. Hodes and D. Cahen, Rain on methylammonium lead iodide based perovskites: possible environmental effects of perovskite solar cells, *J. Phys. Chem. Lett.*, 2015, **6**, 1543–1547.
- 181 M. Ren, X. Qian, Y. Chen, T. Wang and Y. Zhao, Potential lead toxicity and leakage issues on lead halide perovskite photovoltaics, *J. Hazard. Mater.*, 2021, 127848.
- 182 J. Gong, S. Darling and F. You, *Energy Environ. Sci.*, 2015, **8**, 1953.
- 183 J. Wang, Y. Bentley, R. Bentley and L. Feng, How long can the US tight oil boom last, in *Proceedings of the 11th international conference on applied energy (ICAE2019) on August*, 2019, pp. 12–15.
- 184 T. Leijtens, G. E. Eperon, N. K. Noel, S. N. Habisreutinger, A. Petrozza and H. J. Snaith, Stability of metal halide perovskite solar cells, *Adv. Energy Mater.*, 2015, **5**, 1500963.

